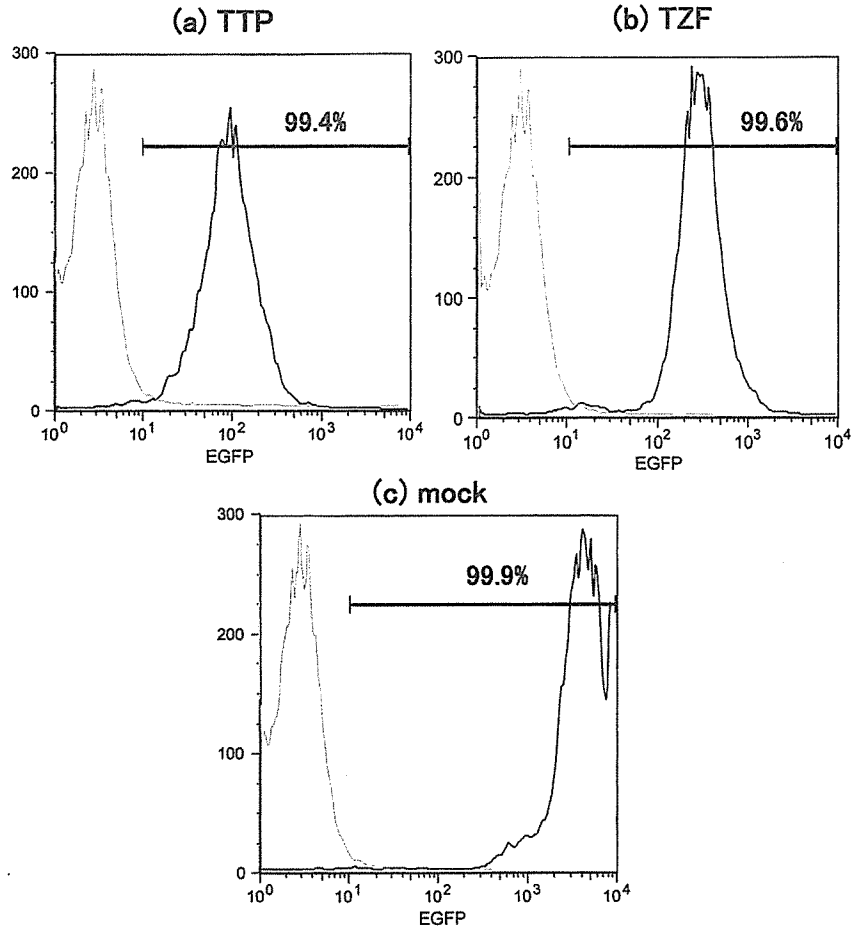

Figure 2. Flow cytometric analysis (a-c) and Western blot analysis (d) of retrovirus vector transduced cells. Jurkat T cells were transduced with retrovirus vector pGCDNsamIRESEGFP containing tristetraprolin (TTP) (a), its tandem zinc finger domain (TZF) gene fragment (b), or no insert (mock) (c). Cell clones were established from transduced cells, and were subjected to flow cytometry. Enhanced green florescent protein (EGFP) was detected in this analysis. Solid line, transduced Jurkat T cells; dotted line, untransduced Jurkat T cells (results representative of three independent clones). Cell lysates were obtained from gene transduced clones and immunoprecipitated (see Materials and methods for details). The immunoprecipitated material was subjected to Western blot analysis using anti-FLAG antibody (d). T, TTP gene transduced Jurkat T cells; Z, TZF gene transduced Jurkat T cells; M, mock-transduced Jurkat T cells; J, untransduced Jurkat T cells; PT, TTP-transfected 293 cells (positive control); PZ, TZF-transfected 293 cells (positive control).

of 1.0×10^6 cells/ml. The supernatant was collected, concentrated five times by using Centricon (Millipore Corporation, Billerica, MA) and stored at -80°C. The concentration of TNF-α was measured using Human TNF-α ready-Set-Go Kit (eBiosience, San Diego, CA), according to the protocol provided by the manufacturer. All assays were performed in duplicate.

Statistical analysis. Student's t-test was used to compare the numbers of TTP- or TZF-transduced Jurkat T cells and mock-transduced Jurkat T cells, and was also used to compare the concentration of TNF-α protein between TTP/TZF-transduced Jurkat T cells and mock-transduced Jurkat T cells. All data were expressed as mean ± SD. A P-value <0.05 denoted the presence of a statistically significant difference.

Results

TTP/TZF gene-containing retrovirus vectors are efficiently transduced into Jurkat T cells. We prepared retrovirus vectors inserted with TTP or TZF encoding genes between the *Not*I and *Sal*I sites as shown in Fig. 1. In these retrovirus vectors, the internal ribosomal entry site (IRES) was present between the inserted genes and the EGFP gene. Thus, the inserted and EGFP genes were translated separately and simultaneously. The percentage of EGFP-positive Jurkat T cells after transduction was 80.8% for TTP-EGFP, 92.5% for TZF-EGFP and 95.6% for the pGCDNsamIRESEGFP vector without any modification (mock-EGFP) (data not shown). The transduced cells were submitted to limiting dilution to obtain cells stably expressing TTP or its active fragment. Obtained clones were assayed for

EGFP expression by flow cytometry, to confirm the efficacy of the limiting dilution. Three clones for TTP- and TZF-transduced cells were established, to rule out the possibility that the results shown hereafter are the consequences of the breakdown of a gene by the insertion of the TTP or TZF genes in a particular clone. The percentages of EGFP expressing cells were 99.4%, 99.6%, and 99.8% for the TTP-, TZF-, and mock-transduced cell clones, respectively (Fig. 2a-c, results representative of three independent clones). However, the fluorescence intensity was highest in mock-transduced cells, followed by TZF-transduced cells, while TTP-transduced cell clones tended to have the lowest fluorescence intensity of all clones established. The cell extracts were immunoprecipitated with anti-FLAG antibody-bound beads, and then subjected to Western blot analyses to confirm that the Jurkat T cells transduced with TTP or TZF retroviral vectors indeed expressed TTP or TZF proteins. The protein extract from Jurkat T cells transduced with the TTP-EGFP retrovirus showed a band at approximately 43 kDa when detected by an anti-FLAG antibody, while that from TZF-EGFP retrovirus-transduced Jurkat T cells showed a band at approximately 15 kDa (Fig. 2d). The estimated molecular weights of recombinant products were in accordance with the sizes of the detected bands. These results indicated that the transduction and limiting dilution procedures were efficiently performed and the proteins were properly expressed.

Introduction of TTP and TZF genes has a small effect on the growth of Jurkat T cells. It is reported that full-length TTP induces apoptosis through the mitochondrial pathway when overexpressed, while TZF does not exhibit such a property (24). To evaluate whether the introduction of the TTP or TZF gene has such an effect on Jurkat T cells, we directly counted the number of cells every day for 5 days to estimate the cell growth (Fig. 3a). At day 5, the mean ± SD number of Jurkat T cells transduced with TTP-EGFP (53.2±20.5 cells/μl) tended to be smaller than that of mock-transduced cells (104.2±23.1 cells/μl) (P=0.0457 by Student's t-test). Cells transduced with TZF-EGFP (65.2±14.0 cells/μl) showed a similar trend, although to a smaller extent (P=0.0665 by Student's t-test). Such tendencies were repeatedly observed in several independent experiments. Next, we detected cells undergoing apoptosis by flow cytometry, using anti-annexin V antibody. The cells were analyzed at both unstimulated and stimulated conditions (final concentration of camptothecin, 6 μg/ml). After 4 h of stimulation, TTP-transduced Jurkat T cells showed the highest percentages of Annexin V-positive cells, suggesting that these cells are more sensitive to camptothecin-induced apoptosis (Fig. 3b).

Introduction of TTP and TZF genes reduces the expression of TNF-α mRNA and the production of TNF-α protein. To evaluate the effect of introducing the TTP or TZF gene into Jurkat T cells, we first measured the amount of TNF-α mRNA in non-stimulated conditions. The expression levels of TNF-α mRNA were lower in TTP-EGFP- and TZF-EGFP-transduced cells, compared with mock-transduced cells (Fig. 4a). However, TNF-α mRNA expression levels were extremely low in all cell groups. Next, we examined the effect of PHA stimulation on those cells. Stimulation of the cells with 5 μg/ml PHA for 1, 6, or 24 h reduced the level of TNF-α mRNA expression in TTP- and TZF-introduced Jurkat T cells at 1 and 6 h after stimulation, compared with mock-transduced cells. In TTP-

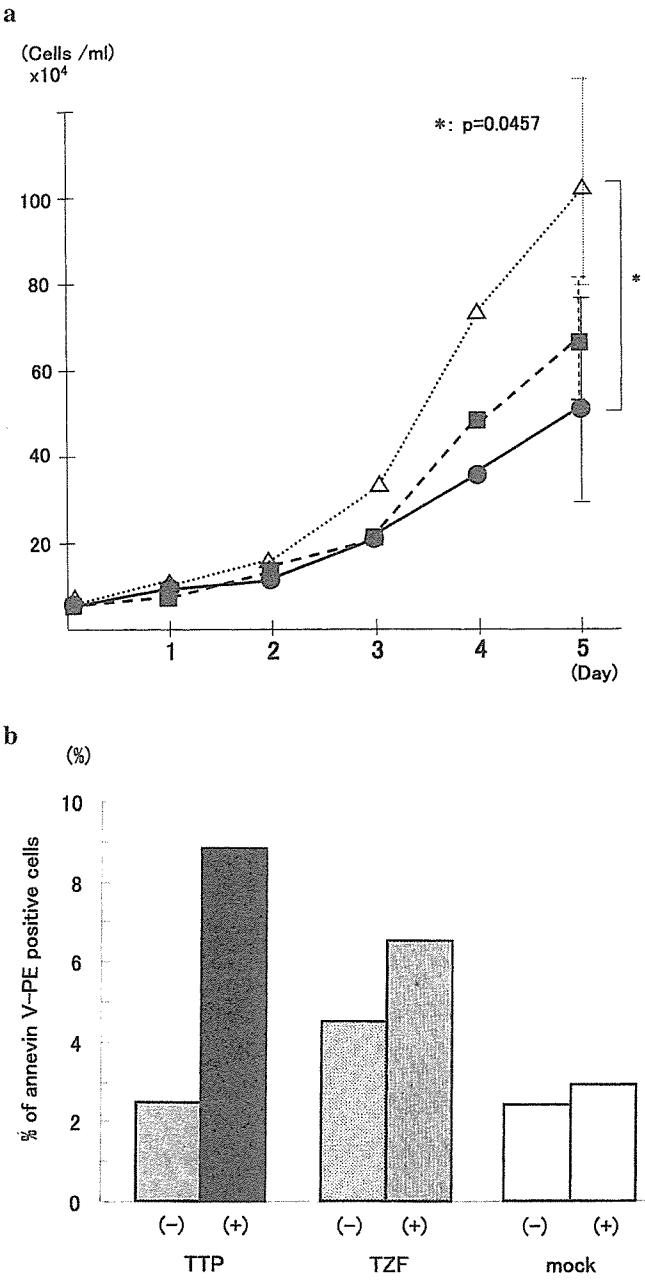

Figure 3. Growth and apoptosis of Jurkat T cells transduced with tristetraprolin (TTP) gene or its tandem zinc finger domain (TZF) gene. (a) Growth of TTP- or TZF-transduced Jurkat T cells. Cells were cultured starting from 1.0×10^5 cells in 3 ml of medium, and the number of live cells was counted daily for 5 days. Results are representative of three independent experiments. Each of the gene-transduced cells were equalized to 3.3×10^4 counts/ml. P-values by Student's t-test. Closed circles, TTP gene-transduced Jurkat T cells; closed squares, TZF gene-transduced Jurkat T cells; open triangles, mock-transduced Jurkat T cells. (b) Induction of apoptosis of TTP- or TZF-transduced Jurkat T cells. Apoptotic cells were detected using phycoerythrin-conjugated anti-annexin V antibody and were analyzed by flow cytometry, either unstimulated, or stimulated with camptothecin (6 μg/ml) for 4 h. Similar results were obtained in three independent experiments. TTP, TTP gene-transduced Jurkat T cells; TZF, TZF gene-transduced Jurkat T cells; mock, mock-transduced Jurkat T cells; (-), unstimulated cells; (+), cells stimulated with camptothecin (6 μg/ml) for 4 h.

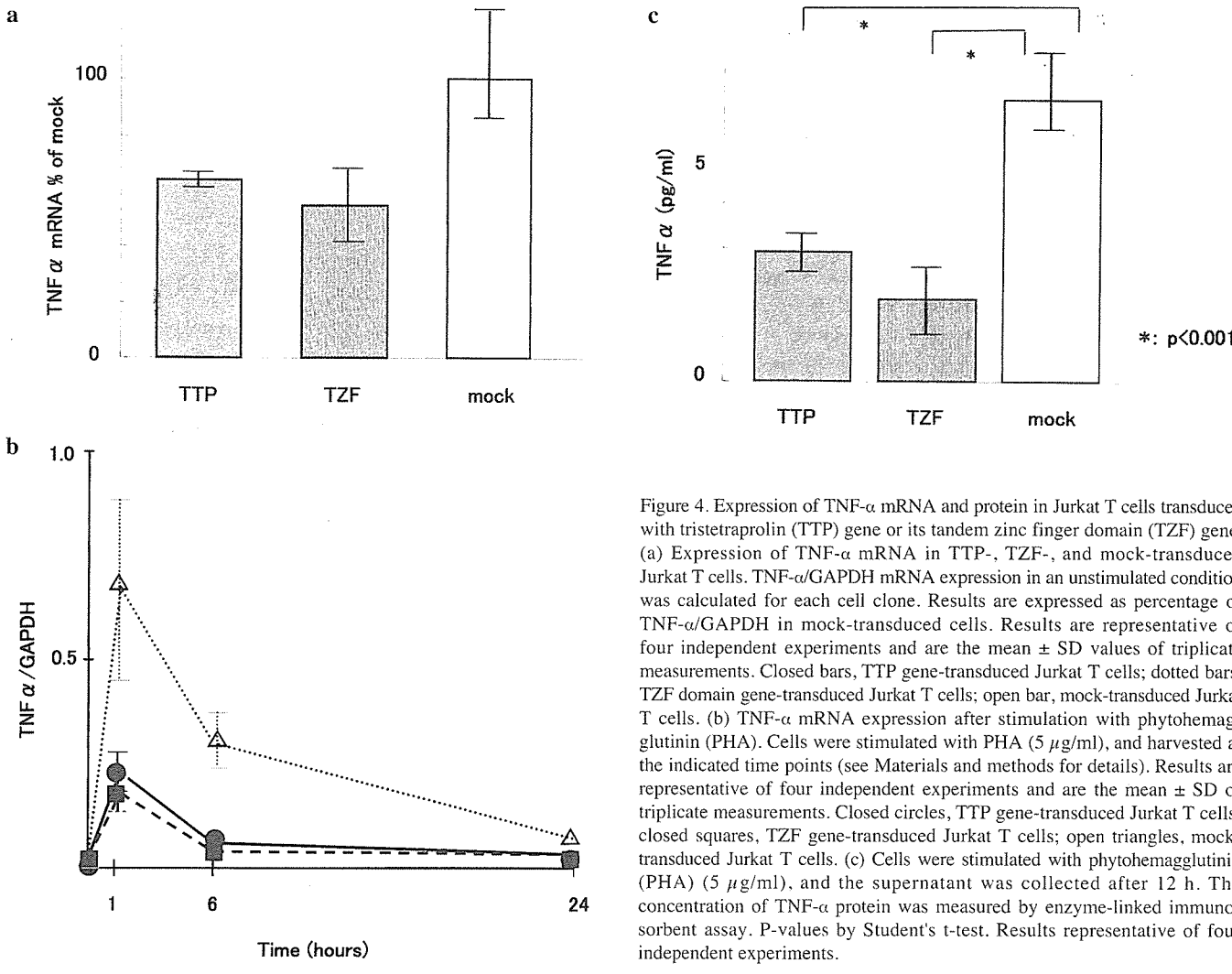

Figure 4. Expression of TNF-α mRNA and protein in Jurkat T cells transduced with tristetraprolin (TTP) gene or its tandem zinc finger domain (TZF) gene. (a) Expression of TNF-α mRNA in TTP-, TZF-, and mock-transduced Jurkat T cells. TNF-α/GAPDH mRNA expression in an unstimulated condition was calculated for each cell clone. Results are expressed as percentage of TNF-α/GAPDH in mock-transduced cells. Results are representative of four independent experiments and are the mean ± SD values of triplicate measurements. Closed bars, TTP gene-transduced Jurkat T cells; dotted bars, TZF domain gene-transduced Jurkat T cells; open bar, mock-transduced Jurkat T cells. (b) TNF-α mRNA expression after stimulation with phytohemagglutinin (PHA). Cells were stimulated with PHA (5 μg/ml), and harvested at the indicated time points (see Materials and methods for details). Results are representative of four independent experiments and are the mean ± SD of triplicate measurements. Closed circles, TTP gene-transduced Jurkat T cells; closed squares, TZF gene-transduced Jurkat T cells; open triangles, mock-transduced Jurkat T cells. (c) Cells were stimulated with phytohemagglutinin (PHA) (5 μg/ml), and the supernatant was collected after 12 h. The concentration of TNF-α protein was measured by enzyme-linked immunosorbent assay. P-values by Student's t-test. Results representative of four independent experiments.

or TZF-transduced cells, TNF-α mRNA expression levels returned to pre-stimulation levels, although the expression level in mock-transduced cells was still high at 6 h after PHA stimulation (Fig. 4b). Similar results were obtained using 2 additional clones for both TTP- and TZF-transduced cells (data not shown). Finally, we measured the amount of TNF-α protein by enzyme-linked immunosorbent assay (ELISA). After 12 h of PHA stimulation, TNF-α protein could be detected, although at low levels. TTP-EGFP- (2.90±0.48) and TZF-EGFP-transduced cells (1.87±0.82) produced significantly less amounts of TNF-α protein, compared with mock-transduced cells (6.33±0.87) (Fig. 4c, $P<0.001$ by Student's t-test).

TTP/TZF gene transduction affects GM-CSF but not c-myc mRNA expression. It is reported that similar to TNF-α mRNA, the expression of GM-CSF mRNA is regulated by ARE binding proteins (20). Thus, we quantified the GM-CSF mRNA expression levels with the same cDNA samples. The expression levels of GM-CSF mRNA were extremely low in all cell groups before PHA stimulation. The GM-CSF mRNA expression level of TTP-EGFP-transduced cells was slightly higher than TZF-EGFP- or mock-transduced cells at 1 h after PHA stimulation. Similar to TNF-α, the expression levels of GM-CSF mRNA in mock-transduced cells were higher than in TTP-EGFP- and TZF-EGFP-transduced cells at 6 and 24 h after PHA stimulation. GM-CSF mRNA expression levels returned to pre-stimulation levels by 24 h after PHA stimulation in TTP-EGFP- and TZF-EGFP-transduced cells (Fig. 5a). As a control, we measured the expression of c-myc mRNA, which is not influenced by regulation though ARE (28). The expression levels of c-myc mRNA in mock-transduced cells tended to be slightly lower at all time points compared with TZF-EGFP-transduced cells, which showed low expression levels at only 6 and 24 h after PHA stimulation. Unlike TNF-α and GM-CSF, we could not detect clear differences in c-myc mRNA expression among TTP-, TZF- and mock-transduced Jurkat T cells (Fig. 5b). Similar results were obtained using 2 additional clones for both TTP- and TZF-transduced cells (data not shown).

Discussion

The importance of TNF-α in the pathogenesis of RA is well-established, and the results of our recent study indicating that the expression level of the TTP gene in the synovial tissues correlates with the severity of RA (25), prompted us to conduct this study to determine whether TTP has the potential to

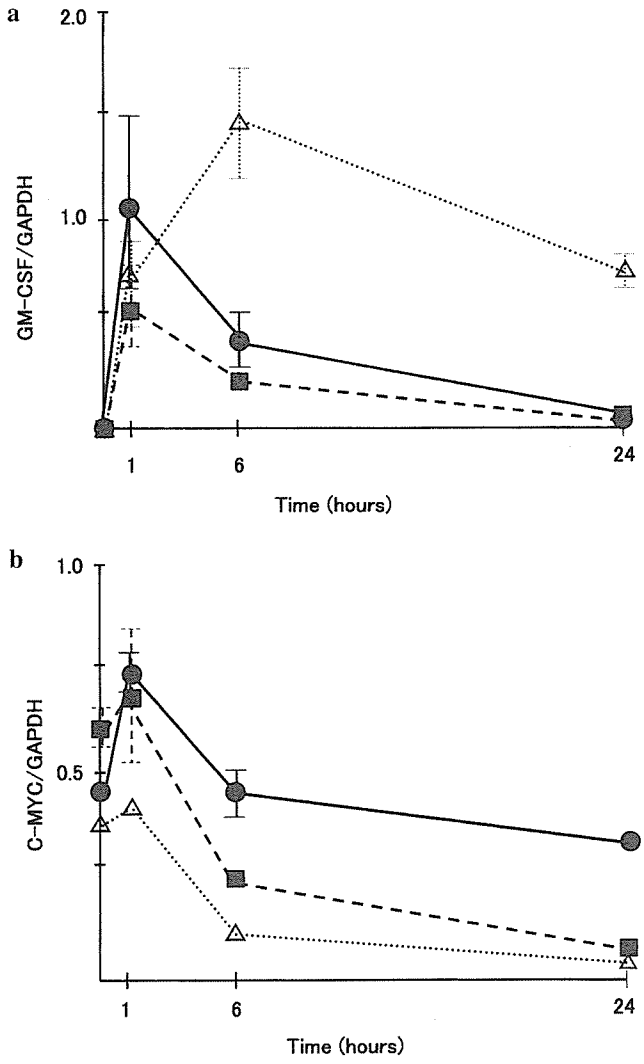

Figure 5. Expression of granulocyte-macrophage colony-stimulating factor (GM-CSF) and c-myc mRNAs in Jurkat T cells transduced with the tristetraprolin (TTP) gene or its tandem zinc finger domain (TZF) gene. (a) Expression of GM-CSF mRNA in TTP- and TZF-transduced Jurkat T cells. Cells were stimulated with phytohemagglutinin (PHA) (5 μg/ml), and harvested at the indicated time points (see Materials and methods for details). Results are representative of four independent experiments and are the mean ± SD values of triplicate measurements. Closed circles, TTP gene-transduced Jurkat T cells; closed squares, TZF gene-transduced Jurkat T cells; open triangles, mock-transduced Jurkat T cells. (b) Expression of c-myc mRNA in TTP- and TZF-transduced Jurkat T cells. Cells were stimulated with PHA (5 μg/ml), and harvested at the indicated time points (see Materials and methods for details). Results are representative of four independent experiments and are the mean ± SD of triplicate measurements. Closed circles, TTP gene-transduced Jurkat T cells; closed squares, TZF gene-transduced Jurkat T cells; open triangles, mock-transduced Jurkat T cells.

become a possible therapeutic target for RA in the future. The main purpose of this study was to investigate whether TTP and TZF can reduce the production of TNF-α by Jurkat T cells.

In this study, we used retrovirus vectors inserted with the EGFP gene as a tool of gene transduction into Jurkat T cells. Retrovirus vectors have been used in human gene therapies for adenosine deaminase deficiency (29,30), and improvements have been made to reduce the toxicity and increase the efficacy of gene transduction (31,32). The addition of EGFP enabled us to easily assess the efficacy of gene transduction by flow cytometry or by fluorescent microscopy. Establishment of gene transferred cell clones was also confirmed using fluorescent microscopy. This enabled us to clearly evaluate the effect of TTP/TZF gene introduction into Jurkat T cells.

We first examined the effect of induction of the TTP gene into Jurkat T cells on cell growth. Johnson and Blackwell (24) reported that TTP protein induces the apoptosis of 3T3 cells, while the TZF protein destabilizes ARE-containing mRNAs, but has no effect on apoptosis. If this observation is applicable to human cells, introduction of the entire TTP gene into human cells may induce apoptosis of these cells. By directly counting the number of cells daily for 5 days, we found that both TTP- and TZF-transduced Jurkat T cells showed a slower growth rate compared to mock-transduced cells (Fig. 3). The cause of growth retardation in TTP- and TZF-overexpressing cells is not clear, but may reflect some ongoing apoptosis of these cells. To verify this assumption, we examined the ratio of cells undergoing apoptosis by flow cytometry, using an anti-annexin V antibody. When stimulated with camptothecin, the ratio of cells undergoing apoptosis was higher in TTP-transduced cells, compared with TZF- and mock-transduced cells. These results suggest that the introduction of the entire TTP molecule may render the cells prone to stimuli that enhance apoptosis. This conclusion is in agreement with the findings of Johnson and Blackwell (24) who reported that multiple TTP sequence domains are required to induce apoptosis.

We next investigated the expression of TNF-α mRNA in each transduced Jurkat T cell clone by using the TaqMan real-time PCR method. Upon stimulation with PHA, TTP-EGFP- and TZF-EGFP-transduced Jurkat T cells expressed less TNF-α mRNA and produced less protein than mock-transduced cells, as expected (Fig. 4). This result suggests that, similar to its mouse counterpart, the TZF region of human TTP can also destabilize TNF-α mRNA. There was no significant difference between TTP- and TZF-transduced cells in TNF-α protein production. Considered with the findings of previous reports on the functions of TTP, these results strongly imply that the TZF region of the TTP protein is sufficient to bind to the 3' ARE region of TNF-α production in Jurkat T cells. The suppressive effect of TTP- and TZF-overexpression on TNF-α production was observed without any serious toxic effects to the cells.

We also investigated the effects of TZF- and TTP-over-expression on other genes that encode ARE-containing mRNAs. AREs are categorized into three classes and the effects on gene regulation by ARE binding protein vary among classes (18,28). The ARE of TNF-α belongs to class II, TTP binds and exerts its function mainly on class II ARE (18,33). Other molecules that contain class II AREs in their mRNA include GM-CSF and interleukin-3 (IL-3) (28,34). On the other hand, molecules such as c-myc, and c-fos have class I AREs (28). To assess the specificity of the effect of TTP- and TZF-overexpression, we analyzed the expression of GM-CSF and c-myc mRNA expression upon PHA stimulation, and compared them with the expression of TNF-α mRNA. Similar to the results of TNF-α mRNA, PHA stimulation reduced the increment of GM-CSF mRNA in TTP- and TZF-transduced cells compared with mock-transduced cells. However, such an effect was delayed compared with that of TNF-α. A previous study indicated that the half-life of GM-

CSF mRNA expressed in T cells was extended when the cells were stimulated by 12-O-tetradecanoyl-phorbol-13 acetate (35). These differences in the time course of mRNA expression may be due to the contribution of other ARE binding proteins such as HuR. HuR also binds to the AREs present in mRNA of a number of genes including TNF-α and GM-CSF, but has a stabilizing effect on these mRNAs (36). A balance of stabilizing and destabilizing ARE binding proteins critically influences the expression of mRNA at the post-transcriptional level (28,37). In contrast, ARE in the mRNA of c-myc belongs to the class I family of AREs. The level of c-myc mRNA expression was not significantly different in TTP-, TZF- and mock-transduced Jurkat T cells. These results indicated that TTP could select the type of AREs to bind, in agreement with a previous report (22), and also that, in addition to the entire TTP molecule, the TZF region of the TTP molecule can exert this function as well. Unlike other studies that used cells with artificially introduced class II ARE-containing mRNAs, our study was performed using Jurkat T cells, which naturally produce TNF-α and GM-CSF. Thus, our data are obtained from a more physiological condition, and will aid in the understanding of the functions and role of post-transcriptional regulation of TNF-α production in humans.

Currently, there are several therapeutic options for RA (38). Biological drugs have been introduced into clinical practice in recent years and have shown dramatic effects in many patients who do not respond to conventional therapies. However, there are still limitations in the usage and effects for those drugs (39). Therefore, new strategies for the treatment of RA must be developed in the future, and we consider that TTP is a potential target in such new therapies. Introducing genes encoding TTP or TZF into synovial tissues, or other methods that induce the expression of the TTP gene may be considered as a possible therapeutic option in the future.

To date, there are few reports on gene transduction in monocytes, the primary source of TNF-α in RA, using retroviruses. Our preliminary studies showed that the transduction efficacy of our retrovirus vectors to a macrophagic cell line was not very high (data not shown). It is necessary to improve our methods to overcome this problem.

One problem for considering TTP as a target for therapy against RA is that, although it selectively destabilizes mRNA containing class II AREs in their 3' region, the mRNA of molecules other than TNF-α, such as GM-CSF and IL-3 also have class II ARE motifs (34). TTP or TZF overexpression may affect the production of these molecules as well as TNF-α, and cause undesirable adverse effects. To clarify the general effects of TTP and TZF over-production, the development of TTP or TZF transgenic animals would be helpful. It is also important to determine the effect and the fate of locally injected retrovirus vectors, since injection of those vectors directly into inflamed joints may enable us to attain the desirable effects with little adverse effects.

In conclusion, we have shown that the transduction of genes encoding TTP or TZF in a Jurkat T cells resulted in the reduction of TNF-α mRNA expression and, hence, reduction of TNF-α production by these cells. The importance of TNF-α in the pathogenesis of RA, and as a therapeutic target for RA, is now well established. Thus, TTP may also be considered as a possible target molecule in the future. The finding that the zinc finger region of the TTP molecule can exert its functions is also of importance, as the use of only the essential portion of TTP may aid in avoiding unwanted adverse reactions.

Acknowledgements

We thank Dr Yoshifumi Muraki, Mr. Yusuke Naito, Ms. Yuko Kori, Ms. Sachiko Motoki, and Ms. Hiromi Yuhashi for their assistance in this study.

References

1. Keffer J, Probrt L, Cazlaris H, *et al*: Transgenic mice expressing human tumor necrosis factor: a predictive genetic model of arthritis. EMBO J 13: 4025-4031, 1991.
2. Mori L, Iselin S, De Libero G and Lesslauer W: Attenuation of collagen-induced arthritis in 55 kDa TNF receptor type 1 (TNFR1)-IgG1-treated and TNFR1-deficient mice. J Immunol 157: 3178-3182, 1996.
3. Campbell IK, O'Donnell K, Lawlor KE and Wicks IP: Severe inflammatory arthritis and lymphadenopathy in the absence of TNF. J Clin Invest 107: 1519-1527, 2001.
4. Williams RO, Feldmann M and Maini RN: Anti-tumor necrosis factor ameliorates joint disease in murine collagen-induced arthritis. Proc Natl Acad Sci USA 89: 9784-9788, 1992.
5. Wooley PH, Dutcher J, Widmer MB and Gillis S: Influence of a recombinant human soluble tumor necrosis factor receptor FC fusion protein on type II collagen-induced arthritis in mice. J Immunol 151: 6602-6607, 1993.
6. Eliott MJ, Maini RN, Feldmann M, *et al*: Treatment of rheumatoid arthritis with chimeric monoclonal antibodies to tumor necrosis factor alpha. Arthritis Rheum 36: 1681-1690, 1993.
7. Holloway AF, Rao S and Shannon MF: Regulation of cytokine gene transcription in the immune system. Mol Immunol 38: 567-580, 2001.
8. Baldwin AS Jr: The transcription factor NF-κB and human disease. J Clin Invest 107: 3-6, 2001.
9. Tak PP and Firestein GS: NF-κB: a key role in inflammatory disease. J Clin Invest 107: 7-11, 2001.
10. Palanki MS: Inhibition of AP-1 and NF-kappa B mediated transcriptional activation: therapeutic potential in autoimmune diseases and structural diversity. Curr Med Chem 9: 219-227, 2002.
11. Clark A: Post-transcriptional regulation of pro-inflammatory gene expression. Arthritis Res 2: 172-174, 2000.
12. Anderson P: Post-transcriptional regulation of tumor necrosis factor α production. Ann Rheum Dis 59 (suppl 1): I3-I5, 2000.
13. Carballo E, Lai WS and Blackshear PJ: Feedback inhibition of macrophage tumor necrosis factor-alpha production by tristetraprolin. Science 281: 1001-1005, 1998.
14. Zhang T, Kruys V, Huez G and Gueydan C: AU-rich element-mediated translational control: complexity and multiple activities of trans-activating factors. Biochem Soc Trans 30: 952-958, 2002.
15. Kontoyiannis D, Pasparakis M, Pizarro TT, Cominelli F and Kollias G: Impaired on/off regulation of TNF biosynthesis in mice lacking TNF AU-rich elements: implications for joint and gut-associated immunopathologies. Immunity 10: 387-398, 1999.
16. Taylor GA, Lai WS, Oakey RJ, *et al*: The human TTP protein: sequence, alignment with related proteins, and chromosomal localization of the mouse and human genes. Nucleic Acids Res 19: 3454, 1991.
17. Taylor GA, Carballo E, Lee DM, *et al*: A pathogenetic role for TNF-α in the syndrome of cachexia, arthritis, and autoimmunity resulting from tristetraprolin deficiency. Immunity 4: 445-454, 1996.
18. Blackshear PJ: Tristetraprolin and other CCCH tandem zinc-finger proteins in the regulation of mRNA turnover. Biochem Soc Trans 30: 945-952, 2002.
19. Anderson P, Phillip K, Stoecklin G and Kedersha N: Post-transcriptional regulation of proinflammatory proteins. J Leukoc Biol 76: 42-47, 2004.
20. Carballo E, Lai WS and Blackshear PJ: Evidence that tristetraprolin is physiological regulator of granulocyte-macrophage colony-stimulating factor messenger RNA deadenylation and stability. Blood 95: 1891-1899, 2000.

21. Lai WS, Carballo E, Strum JR, Kennington EA, Phillips RS and Blackshear PJ: Evidence that tristetraprolin binds to AU-rich elements and promotes the deadenylation and destabilization of tumor necrosis factor alpha mRNA. Mol Cell Biol 19: 4311-4323, 1999.
22. Lai WS, Carballo E, Thorn JM, Kennington EA and Blackshear PJ: Interaction of CCCH zinc finger proteins with mRNA. J Biol Chem 275: 17827-17837, 2000.
23. Johnson BA, Geha M and Blackwell TK: Similar but distinct effects of the tristtraprolin/TIS11 immediate-early proteins on cell survival. Oncogene 19: 1657-1664, 2000.
24. Johnson BA and Blackwell TK: Multiple tristetraprolin sequence domains required to induce apoptosis and modulate response to TNFα through distinct pathways. Oncogene 21: 4237-4246, 2002.
25. Tsutsumi A, Suzuki E, Adachi Y, *et al*: Expression of tristetraprolin (G0S24) mRNA, a regulator of tumor necrosis factor-a production, in synovial tissues of patients with rheumatoid arthritis. J Rheumatol 31: 1044-1049, 2004.
26. Suzuki A, Obi K, Urabe T, *et al*: Feasibility of *ex vivo* gene therapy for neurological disorders using the new retroviral vector GCDNsap packaged in the vesicular stomatitis virus G protein. J Neurochem 82: 953-960, 2002.
27. Iwama A, Osawa M, Hirasawa R, *et al*: Reciprocal roles for CCAAT/enhancer binding protein (C/EBP) and PU.1 transcription factors in Langerhans cell commitment. J Exp Med 195: 547-558, 2002.
28. Raghavan A, Robison RL, McNabb J, Miller CR, Williams DA and Bohjanen PR: HuA and tristetraprolin are induced following T cell activation and display distinct but overlapping RNA binding specificities. J Biol Chem 276: 47958-47965, 2001.
29. Onodera M, Ariga T, Kawamura N, *et al*: Successful peripheral T-lymphocyte-directed gene transfer for a patient with severe combined immune deficiency caused by adenosine deaminase deficiency. Blood 91: 30-36, 1998.
30. Onodera M, Nelson DM, Sakiyama Y, Candotti F and Blaese RM: Gene therapy for severe combined immunodeficiency caused by adenosine deaminase deficiency: improved retroviral vectors for clinical trails. Acta Haematol 101: 89-96, 1999.
31. Ory DS, Neugeboren BA and Mulligan RC: A stable human-derived packing cell line for production of high titer retrovirus/vesicular stomatitis virus G pseudotypes. Proc Natl Acad Sci USA 93: 11400-11406, 1996.
32. Robbins PD and Ghivizzani SC: Viral vectors for gene therapy. Pharmacol Ther 80: 35-47, 1998.
33. Stoecklin G, Stoeckle P, Lu M, Huehlemann O and Moroni C: Cellular mutants define a common mRNA degradation pathway targeting cytokine AU-rich elements. RNA 7: 1578-1588, 2001.
34. Lai WS, Kennington EA and Blacksher PJ: Interactions of CCCH zinc finger proteins with mRNA: non-binding tristetraprolin mutants exert an inhibitory effect on degradation of AU-rich element-containing mRNAs. J Biol Chem 277: 9606-9613, 2002.
35. Bickell M, Cohen RB and Pluznik DH: Post-transcriptional regulation of granulocyte-macrophage colony-stimulating factor synthesis in murine T cells. J Immunol 145: 840-845, 1990.
36. Atasoy U, Watson J, Patel D and Keene JD: ELAV protein HuA (HuR) can redistribute between nucleus and cytoplasm and is upregulated during stimulation and T cell activation. J Cell Sci 111: 3145-3156, 1998.
37. Lu JY and Schneider RJ: Tissue distribution of AU-rich mRNA-binding proteins involved in regulation of mRNA decay. J Biol Chem 279: 12974-12979, 2004.
38. Weinblatt ME: Treatment of rheumatoid arthritis. In: Arthritis and Allied Conditions: A Textbook of Rheumatology. 13th edition. Koopman WJ (ed). Williams & Wilkins, Baltimore, MD, pp1131-1141, 1997.
39. Taylor PC: Anti-TNF alpha therapy for rheumatoid arthritis: An update. Intern Med 42: 15-20, 2003.

T cell receptor BV gene repertoire of lymphocytes in bronchoalveolar lavage fluid of polymyositis/dermatomyositis patients with interstitial pneumonitis

YUSUKE CHINO[1], HIDEYUKI MURATA[1], DAISUKE GOTO[1], ISAO MATSUMOTO[1], AKITO TSUTSUMI[1], TOHRU SAKAMOTO[2], MORIO OHTSUKA[2], KIYOHISA SEKISAWA[2], SATOSHI ITO[1] and TAKAYUKI SUMIDA[1]

Divisions of [1]Rheumatology, and [2]Pulmonary Medicine,
Department of Internal Medicine, University of Tsukuba, Tsukuba City, Japan

Received July 25, 2005; Accepted August 30, 2005

Abstract. We analyzed the T cell receptor (TCR) repertoire of bronchoalveolar lavage fluid (BALF) lymphocytes from polymyositis (PM) and dermatomyositis (DM) patients with interstitial pneumonitis (IP) to elucidate the pathogenic mechanisms of IP in these disorders. Samples from 2 PM patients, 1 DM patient and 3 healthy controls were used. RNA was isolated from BALF, cDNAs were synthesized, and family PCR and Southern blot analysis were performed by primers specific for TCR BV1-25 and TCR BC to determine TCR repertoire. We examined single-strand conformation polymorphism (SSCP) to evaluate T cell clonality. The CDR3 region of TCR BV genes in BALF T cells were determined by DNA sequencer. Our examination showed that TCR repertoire of T cells in BALF was heterogeneous both in patients with PM/DM and control subjects. SSCP analysis demonstrated an increased number of accumulated T cell clones in BALF of three PM/DM patients, but not in the healthy subjects and the junctional sequence analysis showed the presence of conserved amino acid motifs (RGS, GLA, LQG, SGG, DRG, GTS, TSGR, GGS, GQA, GAG, GTG) in the TCR-CDR3 region of BALF lymphocytes from PM/DM patients, which were not detected in the control. Our findings suggest that T cells in BALF may recognize the restricted antigen and accumulate via antigen-driven stimulation, suggesting that T cells may play a crucial role in the development of IP in patients with PM/DM.

Correspondence to: Professor Takayuki Sumida, Division of Rheumatology, Department of Internal Medicine, University of Tsukuba, 1-1-1 Tennodai, Tsukuba City, Ibaraki 305-8575, Japan
E-mail: tsumida@md.tsukuba.ac.jp

Abbreviations: PM/DM, polymyositis/dermatomyositis; IP, interstitial pneumonitis; SSCP, single-strand conformation polymorphism; TCR, T cell receptor; BALF, bronchoalveolar lavage fluid

Key words: interstitial pneumonitis, polymyositis, dermatomyositis, T cell receptor, bronchoalveolar lavage fluid lymphocytes, T cell clones, amino acid motifs

Introduction

Polymyositis (PM) and dermatomyositis (DM) are systemic inflammatory disorders that affect skeletal muscles and various other organ systems including the lungs. Pulmonary interstitial lung disease (ILD) is the most frequent pulmonary pathological finding recognized to be associated with PM/DM. Recent advances in biotechnology in the field of bronchoalveolar lavage (BAL) have provided considerable information on the alveolar cellular components in PM/DM with IP (1). Pulmonary damage and fibrosis represent the consequences of immune response and inflammatory process. Previous studies showed that lymphocytes, especially T cells, and alveolar macrophages play a central role in the pathogenesis of PM/DM with IP, although the mechanism that triggers these cells has not been elucidated (2).

T cells recognize antigens in the context of major histocompatibility complex (MHC) on antigen-presenting cells (APC) through an antigen receptor, the T cell receptor (TCR). Several groups investigating TCR genes in autoimmune diseases such as rheumatoid arthritis (3), Sjögren's syndrome (4,5), and multiple sclerosis (6,7) among other diseases, have demonstrated that T cells accumulate oligoclonally in the inflammatory lesions. Furthermore, conserved amino acid motifs have been observed in the CDR3 region of TCR gene, but no skewed usage of TCR genes (6,7).

Several studies have examined TCR genes of BAL fluid (BALF) T cells in patients with various lung diseases such as sarcoidosis, bronchial asthma, and idiopathic pulmonary fibrosis (IPF). Moller and colleagues (8) demonstrated an increased number of TCR BV8 T cells in BALF of patients with sarcoidosis. Zissel *et al* (9) showed the predominant usage of TCR BV5, BV8, BV12, BV13S3, and BV19 genes in BALF. Bellocq and coworkers (10) found a number of TCR BV19-positive T cells in BALF of patients with sarcoidosis. In asthmatic patients, Hodges *et al* (11) reported expansion of TCR BV5S2/3-positive T cells in BALF. In contrast, there

Table I. Characteristics of study population.

	Patients			Healthy subjects		
	DM-I	PM-1	PM-2	HS-1	HS-2	HS-3
Age (years)	57	57	50	52	32	28
Sex	F	F	F	M	M	M
Smoking	-	-	-	+	+	-
% vital capacity (% predicted value)	102.7	81.4	66.8	ND	118.0	133.4
FEV1 %	93.5	73.1	100.0	ND	80.5	97.4
% DLco	58.1	42.3	45.2	ND	91.7	90.9
PaO_2 (mmHg)	68.0	75.4	100.5	ND	ND	ND
Chest radiograph						
Diffuse reticular infiltrate pattern	±	+	+	-	-	-
BAL analysis						
Total cell count ($x10^5$/ml)	350	3.8	6.1	1	2.6	0.8
Differential count (%)						
Macrophages	57.7	43.1	77.5	90.5	93.0	90.0
Lymphocytes	41.0	14.7	18.1	3.2	3.5	8.0
Neutrophils	1.3	43.1	4.2	4.9	3.0	2.0
Eosinophils	0.0	7.3	0.2	1.4	0.5	0
CD4/CD8 ratio	0.6	0.3	0.4	2.2	0.6	4.7
Absolute number of lymphocytes[a]	1435.0	5.6	11.0	0.3	0.9	0.6

The diagnosis of PM/DM was based on clinical criteria for PM/DM of Bohan and Peter (22). [a]In $x10^4$/ml.

was no dominant usage of TCR BV genes in BALF T cells in patients with non-atopic asthma (12). We also reported conserved amino acid motifs in the CDR3 region of the TCR BV genes in clonally expanded BALF T cells of patients with IPF (13). These findings support the hypothesis that BALF T cells of patients with sarcoidosis, atopic bronchial asthma, and IPF may be induced by antigens on antigen-presenting cells. To our knowledge, there are no reports on the TCR gene of BALF T cells, or possible triggering factors, in patients with IP associated with PM/DM.

The present study was conducted to investigate the pathogenesis of IP in PM/DM and analyze the TCR BV repertoire and clonality of T cells infiltrating the lungs. The results showed oligoclonal expansion of T cells in BALF of patients with IP in PM/DM, suggesting antigen-driven stimulation. Furthermore, highly conserved amino acid sequence motifs were identified in the TCR BV CDR3 region of accumulated BALF T cells. The results indicate that BALF T cells in PM/DM patients with IP recognize a limited epitope on antigens. Based on these findings, we discuss possible pathogenic mechanisms of IP associated with PM/DM.

Materials and methods

Patients and histopathological examination. Two patients with PM and 1 patient with DM were referred to Tsukuba University Hospital. Each patient met the criteria for PM or DM diagnosis, including clinical features, laboratory findings, chest X-ray and chest CT findings, and endoscopic biopsies. We also recruited three healthy subjects who had no respiratory-related complaints and negative chest X-ray films. The clinical characteristics of the 3 patients with PM/DM and healthy subjects are summarized in Table I. Written informed consent was obtained from all patients. A transbronchial lung biopsy was performed, and the tissue was stained with hematoxylin and eosin. No open lung biopsy was performed.

Bronchoalveolar lavage and peripheral blood lymphocytes. BAL was performed on the involved lung segment (right lower lobe and posterior segment) of the 3 patients with IPF and three healthy control subjects. After topical anesthesia, the fiberoptic bronchoscope (Olympus type BF20, Olympus Co., Tokyo, Japan) was advanced into the described segment and wedged, and 50 ml sterile 0.9% saline at 37°C was injected through the bronchoscope. The latter process was performed three times. The volume of BALF recovered from the involved segment was approximately 100 ml. Cells in BALF were passed through sterile gauze to remove debris. BALF from patients was centrifuged at 20 x g and 4°C for 10 min, and washed twice with phosphate-buffered saline (PBS). Following cell count, part of the cell mass was subjected to flow cytometric analysis. A number of cells

($2x10^5$) were stained with monoclonal antibodies (mAbs) against Leu 4 (anti-CD3), Leu 3a (anti-CD4), and Leu 2a (anti-CD8) (Becton Dickinson, Mountain View, CA). After flow cytometry, peripheral blood lymphocytes (PBLs) from patients with IP associated with PM/DM were obtained by Ficoll-Hypaque density gradient centrifugation, and immediately analyzed.

Polymerase chain reaction, Southern blot analysis and single-strand conformation polymorphism. Total RNA from BALF cells was prepared with Isogen (Nippon Gene Co., Tokyo). PCR and cDNA synthesis were performed as described previously by Sumida *et al* (4). Briefly, first-strand cDNA was synthesized from 1 μg total RNA in a 20-μl reaction mixture containing an oligo(dT) primer by avian myeloblastosis virus reverse transcriptase. Amplification was performed with *Taq* polymerase in 50 μl standard buffer, using 0.2 μl cDNA (corresponding to 10 ng total RNA), with primers specific for 25 different TCR BV genes and BC gene. The sequences of the primers were obtained from previously published data (5). Denaturing was performed at 95˚C for 1.5 min, annealing at 60˚C for 1.0 min, and extension at 72˚C for 1.0 min, for 30 cycles in a DNA Thermal Cycler (Perkin-Elmer Corp., Norwork, CT). One-tenth of each amplified PCR product was subjected to 2% agarose gel electrophoresis and transferred to a nylon membrane. Membranes were further hybridized with digoxygenin-labeled TCR BC probe, and visualized using the DIG luminescent detection kit (Boehringer Mannheim, Mannheim, Germany). The digoxygenin-labeled TCR BC probe was synthesized employing the PCR DIG probe synthesis kit (Boehringer Mannheim), with 5'-TCR BC (5'-GAGGATCTGAGAAATGTGACT-3') and 3'-TCR BC (5'-CAAGCACACACGAGGGTAGCCT-3') primers. For individual single-strand conformation polymorphism (SSCP) assays, amplified DNA was diluted (1:20) in a denaturing solution [95% formamide, 10 mM ethylenediaminetetraacetic acid (EDTA), 0.1% bromophenol blue, 0.1% xylene cyanol] at 90˚C for 2 min. Diluted samples (2:1) were subjected to electrophoresis in non-denaturing 5% polyacrylamide gels containing 10% glycerol (14). Gels were run at 35 W constant power for 2 h. Following electrophoresis, DNA was transferred to Immobilon-S (Millipore Intertech, Bedford, MA), and hybridized with biotinylated TCR BC probe [5'-A (AC) AA (GC) GTGTTCCCACCCGAGGTCGCTGTGTT-3'], streptavidin, biotinylated alkaline phosphatase, and a chemiluminescent substrate system (Plex™ Luminescence kit, Millipore).

Sequencing of cDNA encoding TCR BV genes. Complementary DNA, encoding TCR BV genes from BALF and PBLs, was purified from polyacrylamide gels for SSCP, and amplified by PCR using the primers described above. PCR products were ligated to plasmids using the TA cloning kit (Invitrogen, San Diego, CA, USA), transformed into competent INVαF' *Escherichia coli* cells, and grown under appropriate conditions. After selection of TCR BC-positive colonies, plasmid DNA was purified by alkaline lysis for DNA sequencing. Sequencing reactions were performed using an automated DNA sequencer (model 377A, Applied Biosystems, Foster City, CA).

Results

Heterogeneous TCR BV repertoire of BALF T cells in patients with IP associated with PM/DM. The mean number of lymphocytes was significantly higher in BALF of PM/DM with IP patients (5,300,000/ml) compared with the control (6,200/ml). The majority of expanded lymphocytes were $CD8^+$ T cells, because CD4/CD8 ratio was decreased in PM/DM + IP to 0.43 from 2.5 in the control. To analyze the pathogenesis of IP associated with PM/DM, we examined the TCR repertoire of BALF T cells from the three patients (DM-1, PM-1, and PM-2) using the family PCR method. PBLs from identical patients were used as a control. Table I lists the clinical profiles of PM/DM patients with IP. Chest CT revealed diffuse reticulonodular opacities, honey combing and ground-glass attenuation. Histopathological examination of lung biopsies from these patients showed a large number of mononuclear cells in the inflamed alveolar septa. The pathological changes in the interstitial septa, alveolar spaces, bronchial mucosa, and pleura were similar to those in the lungs of usual interstitial pneumonia (UIP). No infectious agents or parasites were observed, and there was no evidence of vasculitis. TCR analysis showed expression of the majority of TCR BV family genes in both BALF T cells and PBL in all patients (data not shown). These results suggest that the TCR BV repertoire of T cells in the lung is heterogeneous and that there is no restricted predominant usage of TCR BV genes.

Lung-specific T cell clones in patients with IP associated with PM/DM. TCR BV genes in BALF and peripheral T cells were examined by PCR-SSCP in order to investigate the clonality of pulmonary T cells in patients with IP associated with PM/DM. Fig. 1 depicts lung-specific bands that were found in several TCR BV genes of the three IP patients with PM/DM. These bands were detected in TCR BV2, 3, 4, 5, 6, 8, 9, 10, 11, 12, 13, 16, 17, 19, 20, 23, 24, and 25 genes. The number of bands encoding TCR BV genes in the lung is summarized in Table II. We observed a significant increase in the number of expanded clones in BALF of three IP patients (27, 23 and 21 clones), compared with three healthy subjects (6, 9 and 8 clones) ($p<0.05$). These results indicate accumulation of some T cells in the lungs of PM/DM patients with IP, suggesting that these cells proliferate by antigen stimulation.

Conserved amino acid sequence motifs in the CDR3 region of TCR BV genes from BALF-specific T cells of IP associated with PM/DM. To examine the amino acid sequences of the CDR3 region in the TCR BV gene, we focused on the lung-specific T cell clones by SSCP analysis. DNAs encoding the TCR BV genes from BALF-specific bands were eluted from gels, followed by sequencing the corresponding CDR3 regions. As shown in Table III, the CDR3 region of the lung-specific accumulated T cell clones contained conserved amino acid motifs. In DM-1 patient, RGS, GLA, LQG, SGG, DRG, and GTS motifs were found in BV2-1, BV19-2 and BV20-3, BV5-1 and BV10-1, BV9-2 and BV13-3, BV10-2 and BV24-2, BV13-2 and BV20-3, and BV9-3 and BV24-2 clones, respectively. In PM-1 patient, TSGR, GGS, GQA, GAG motifs were found in BV4-2 and BV12-1, BV8-2 and

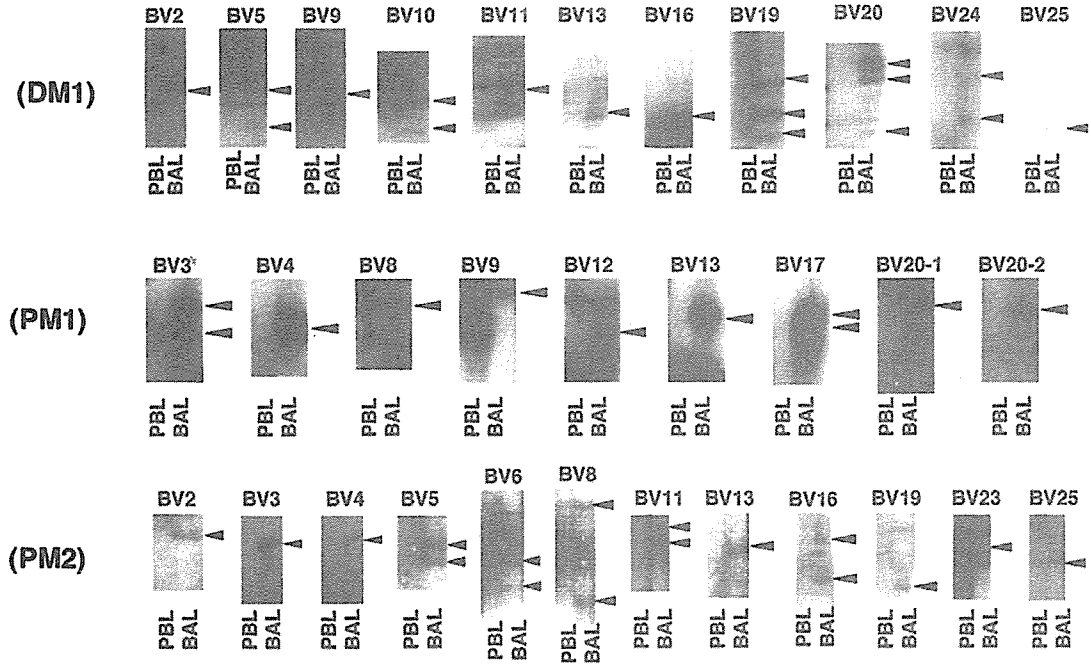

Figure 1. BALF-specific T cell clones. SSCP on TCR BV1-25 genes were carried out using cDNA from BALF and PBL of PM/DM patients and healthy subjects. Arrowheads show BALF-specific T cell clones.

Table II. Accumulated T cell clones in BALF of patients with PM/DM + IP.

TCR BV gene	1	2	3	4	5	6	7	8	9	10	11	12	13	14	15	16	17	18	19	20	21	22	23	24	25	Total
DM-1	0	1	0	0	2	0	0	0	3	5	1	0	3	0	0	3	0	0	3	3	0	0	0	2	1	27
PM-1	0	0	4	2	0	0	0	2	2	0	0	3	2	0	0	0	4	0	0	4	0	0	0	0	0	23
PM-2	0	1	1	1	2	2	0	3	0	0	2	0	3	0	0	2	0	0	1	0	0	0	2	0	1	21
HS-1	1	2	0	0	0	0	0	1	0	0	0	0	0	0	0	0	0	0	0	2	-	-	-	-	-	6
HS-2	0	0	0	0	0	1	0	1	0	0	1	0	0	1	1	0	0	1	0	0	0	0	0	1	2	9
HS-3	0	0	1	0	0	0	1	0	0	1	0	0	0	1	0	0	0	1	0	1	1	0	0	1	0	8

Numbers represent T cell clones accumulated in BAL of patients with PM/DM + IP. The distinct bands encoding TCR BV genes on SSCP were described as the number of BAL-specific T cell clones. -, not done.

BV20-1, BV9-2 and BV20-3, and BV12-3 and BV17-1 clones, respectively. In PM-2 patient, GTG motif was found in BV8-2 and BV16-2 clones, respectively (Table III). In contrast, BALF-specific bands of the healthy subjects did not reveal any conserved amino acid motifs in the CDR3 region (Table IV). The conserved amino acid motifs in the CDR3 region of TCR are summarized in Table V. These findings suggest that accumulated T cells in the lungs of patients with IP associated with PM/DM recognize a limited epitope on antigens.

Discussion

Recent studies on TCR of PBL and T cells infiltrating into muscles showed clonal expansion of $CD8^+$ T cells in peripheral blood and muscles, although the TCR repertoire was heterogeneous (15-21). In contrast, there are no studies on TCR of BALF T cells of PM/DM patients with IP. In the present study, we analyzed the TCR repertoire and sequences of TCR CDR3 regions and determined that the TCR BV repertoire was not skewed, but there were conserved amino acids in the CDR3 region in BALF T cells of PM and DM patients. We speculate that some T cells recognize the antigen in the context of HLA molecule and trigger autoimmune reaction. These results are similar to those reported in patients with IPF (13) but not those with sarcoidosis and atopic asthma (9-11).

The conserved amino acid sequences in the CDR3 region of BALF T cells of patient DM1 are RGS motif in TCR BV2-1, BV19-2 and BV20-3, GLA motif in TCR BV5-1 and BV10-1, LQG motif in TCR 9-2 and BV13-3, SGG motif in TCR BV10-2 and BV24-2, DRG motif in TCR BV13-2 and

Table III. Conserved amino acid motifs in the CDR3 region of BALF-specific T cells of patients with PM/DM.

A, DM-1

clone	V 92	N-D-N 96	J 106	
BV2-1	C S A	H P R G S P P G	G Y	BJ1S2
BV5-1	C A S S	L G L A F	Q	BJ2S1
BV5-2	C A S S	S T V S	E Q	BJ2S7
BV9-1	C A S S	Q P S E V E	T Q	BJ2S3
BV9-2	C A S S	R K L Q G	T G E L	BJ2S2
BV9-3	C A S S	G T S I S	G Y	BJ1S2
BV10-1	C A	C T G L A K G	Y N E Q	BJ2S1
BV10-2	C A S	P R L S G G	T Q	BJ2S3
BV10-3	C A S	G D	N Q P Q	BJ1S5
BV10-4	C A S S	K S T G R P T	Q	BJ2S7
BV10-5	C A G S	D P G T G	E Q	BJ2S1
BV11-1	C A S	V N T R T F	E A	BJ1S1
BV13-1	C A S S	Y S Q	N Q P Q	BJ1S5
BV13-2	C A S	D D R G	D T Q	BJ2S3
BV13-3	C A S S	L P L Q G	E K L	BJ1S4
BV16-1	C A S S	Y T D G V E	T Q	BJ2S3
BV16-2	C A S	P H I M G A R R	Q	BJ2S3
BV16-3	C A S S	R S G S F	S Y E Q	BJ2S7
BV19-1	C A S S	L R R E	Q P Q	BJ1S5
BV19-2	C A S	R N R G	S Y E Q	BJ2S7
BV19-3	C A S S	Q S R G K R	E Q	BJ2S1
BV20-1	C A W S	R G Q	N E K L	BJ1S4
BV20-2	C A W	R G H R T R I	Q	BJ2S1
BV20-3	C A W	K G D R G S D	Q	BJ2S3
BV24-1	C A T S	S F G G	E T Q	BJ2S5
BV24-2	C A T S	S D S G G T S E	T Q	BJ2S5
BV25-1	C A S	S P G Q P T	Y E Q	BJ2S7

B, PM-1

clone	V 92	N-D-N 96	J 106	
BV3-1	C A S S	A P R D T E A	F F	BJ1S1
BV3-2	C A S S	P P G L R E	P Q	BJ1S5
BV3-3	C A S S	L G Y L	T G E L	BJ2S2
BV3-4	C A S S	P Q K M G T G	Q P Q	BJ2S1
BV4-1	C S A	A S R G	N T E A	BJ1S1
BV4-2	C S V	A G T S G R S	S Y E Q	BJ2S1
BV8-1	C A S S	L R G	S Y N E Q	BJ2S1
BV8-2	C A	N P F R G G S	E Q	BJ2S1
BV9-1	C A S S	A G L	S Y E Q	BJ2S7

Table III. Continued.

B, PM-1

	V				N-D-N								J				
clone	92				96								106				
BV9-2	C	A	S	S			Q	D	W	G	Q	A		N	E	K	L	BJ1S4
BV12-1	C	A	I		S	D	T	S	G	R	G			T	D	T	Q	BJ2S3
BV12-2	C	A	I		S	E	S	L	A						D	T	Q	BJ2S3
BV12-3	C	A	I		S	G	A	G					S	T	D	T	Q	BJ2S3
BV13-1	C	A	S	S			W	S	L	D	R	G	D		N	E	Q	BJ2S1
BV13-2	C	A	S	S			P	S	G	L	P	P		T	D	T	Q	BJ2S3
BV17-1	C	A	S	S			I	G	A	G	V			Y	N	E	Q	BJ2S1
BV17-2	C	A	S		N	A	R	P	F			S	G	A	N	V	L	BJ2S6
BV17-3	C	A	S	S			P	W	T	G	T			N	T	E	A	BJ1S1
BV17-4	C	A	S	S			I	Q	G	R					Q	P	Q	BJ1S5
BV20-1	C	A	W	S			V	G	G	S				S	Y	E	Q	BJ2S7
BV20-2	C	A	W	S			S	T	E							E	Q	BJ2S1
BV20-3	C	A	W	S			G	Q	A	A			S	T	D	T	Q	BJ2S3
BV20-4	C	A	W		G	P	D	I	P						E	T	Q	BJ2S7

C, PM-2

	V				N-D-N								J				
clone	92				96								106				
BV2-1	C	S	A		L	T	N	T						N	E	Q	BJ2S1
BV3-1	C	A	S	S			W	R						T	G	E	L	BJ2S2
BV4-1	C	S	V		V	G	T							T	D	T	Q	BJ2S3
BV5-1	C	A	S		A	R	D	S	G	R	L	R			E	K	L	BJ1S4
BV5-2	C	A	S	S			L	K	E	G	L	G		S	T	D	T	Q	BJ2S3
BV6-1	C	A	S	S			L	D	G	S				N	T	G	E	L	BJ2S2
BV6-2	C	A	S	S			L	G	P						N	Y	G	Y	BJ1S2
BV8-1	C	A	S	S			L	K	D							E	Q	BJ2S7
BV8-2	C	A	S		S	Y	G	T	G						S	Y	E	Q	BJ1S6
BV8-3	C	A	S		T	R	T	D	L						N	T	E	A	BJ1S1
BV11-1	C	A	S		S	L	G	T							N	Y	G	Y	BJ1S2
BV11-2	C	A	S		L	G	G	A	V	T					T	G	E	L	BJ2S2
BV13-1	C	A	S		S	H	D	G	P						N	Y	G	Y	BJ1S2
BV13-2	C	A	S		S	R	G	D	Y	A					N	E	K	L	BJ1S4
BV13-3	C	A	S		R	M	G	Q	G	F						E	Q	BJ2S7
BV16-1	C	A	S	S			P	G	G	N						E	Q	BJ2S7
BV16-2	C	A	S	S			Q	G	V	A	G	T	G	L		E	T	Q	BJ2S5
BV19-1	C	A	S		S	P	S	D	G	T				S	Y	E	Q	BJ2S7
BV23-1	C	A	S	S			S	P	R	T	W	A				Y	Q	BJ2S7
BV23-2	C	A	S	S			Y	N	Y	R	G	A	G	V		T	E	A	BJ1S1
BV25-1	C	A	S	S			Q	S	I	R	G	R				E	Q	BJ2S7

Table IV. CDR3 region of BALF T cells of healthy subjects (HS).

A, HS-1

Clone	V 92							N-D-N 96										J 106				
BV1-1	C	A	S	S				A	G	T					N	Q	E	T	Q	BJ2S5
BV1-2	C	A	S	S				V	T	G	G	S	L				N	E	Q	BJ2S1
BV2-1	C	S	A	K				G	E	R	G	G						E	Q	BJ2S1
BV2-2	C	S	A	R				I	G	T						Q	E	T	Q	BJ2S5
BV2-3	C	S	A				D	R	N							Q	E	T	Q	BJ2S5
BV2-4	C	S	A	S				K	T	G						T	G	E	L	BJ2S2
BV8-1	C	A	S	S				L	G								Y	E	Q	BJ2S7
BV20-1	C	A	W					K	R	E	S							E	Q	BJ2S1
BV20-2	C	A			F	T	G	Q	G	A						S	Y	E	Q	BJ1S5
BV20-3	C	A			S	R	D	R	G	L						N	Q	P	Q	BJ1S5

B, HS-2

Clone	V 92							N-D-N 96										J 106				
BV6-1	C	A	S	S				H	S	G	R	E	R			Y	N	E	Q	BJ2S1
BV8-1	C	A	S			Q	G								M	N	T	E	A	BJ1S1
BV8-2	C	A	S	S			F	G	A									E	Q	BJ2S7
BV8-3	C	A	S	S			F	S	G	T	S	G					N	E	Q	BJ2S1
BV11-1	C	A	S			V	M	M	T	G							T	E	A	BJ1S1
BV11-2	C	A	S			V	T	G	G							T	G	E	L	BJ2S2
BV13-1	C	A	S			S	R	G	D	Y	A					T	D	D	Q	BJ1S4
BV13-2	C	A	S			R	M	G	Q	G	F					T	G	E	L	BJ2S1
BV14-1	C	A	S	S			L	V	G	G	R							E	Q	BJ2S3
BV14-2	C	A	S	S			W	R	G								Y	E	Q	BJ2S2
BV15-1	C	A	T	S			G	P	A	D	E	N	G		S	S	Y	E	Q	BJ2S1
BV15-2	C	A	T	S			D	G										E	Q	BJ2S7
BV18-1	C	A	S	S			P	G	A	G					S	Y	N	E	Q	BJ2S7
BV18-2	C	A	S	S			P	Q	G	G						N	E	K	L	BJ2S1
BV18-3	C	A	S	S			P	P	G	P	L							E	Q	BJ2S1
BV21-1	C	A	S	S			S	Q	G	P	T	G					N	E	Q	BJ2S1
BV24-1	C	A	T	S			R	D	P	T	R							E	Q	BJ2S7

C, HS-3

Clone	V 92							N-D-N 96										J 106				
BV3-1	C	A	S	S				P	E	P	Q	G	V	R				T	Q	BJ2S5
BV7-1	A	A	S			Y	S	S	G								Y	E	Q	BJ2S7
BV7-2	A	A	S	Q			D	G	G	G	G				N	T	G	E	L	BJ2S2
BV10-1	C	A	S	S			S	P	L	G	A							P	Q	BJ1S5
BV10-2	C	A	S	S			K	T	E	R	E						Y	E	Q	BJ2S7
BV14-1	C	A	S	S			L	S	E	M	G						N	E	Q	BJ2S1
BV18-1	C	A	S	S			R	P	G	S	G					T	D	T	Q	BJ2S3
BV18-2	C	A	S	S			Q	T	E								N	I	Q	BJ2S4
BV20-1	C	A	W	S			P	L	A	L							E	T	Q	BJ2S5
BV20-2	C	A	W			A	L	G	I	A	S						N	E	Q	BJ2S1
BV24-1	C	A			S	S	N	T	P	K	A	S	L	V	G	E	T	Q		BJ2S5
BV25-1	C	A	S	S			T	S	G	T	G	D					T	E	A	BJ1S1
BV25-2	C	A	S	S			T	G	T	R	G						T	E	A	BJ1S1

Table V. Summary of conserved amino acid motifs in the TCR CDR3 region.

	RGS	BV2-1, 19-2, 20-3
	GLA	BV5-1, 10-1
	LQG	BV9-2, 13-3
DM-1	SGG	BV10-2, 24-2
	DRG	BV13-2, 20-3
	GTS	BV9-3, 24-2
	TSGR	BV4-2, 12-1
	GGS	BV8-2, 20-1
PM-1	GQA	BV9-2, 20-3
	GAG	BV12-3, 17-1
PM-2	GTG	BV8-2, 16-2

BV20-3, and GTS motif in TCR 9-3 and BV24-2 clones. In contrast, TSGR, GGS, GQA, GQA, GAG, and GTG motifs were found in TCR BV4-2 and BV12-1, BV8-2 and BV20-1, BV9-2 and BV20-3, BV12-3 and BV17-1, and BV8-2 and BV16-2 clones, respectively in patients with PM. These observations are specific for BALF T cells in PM and DM, since the same conserved amino acids motifs were not found in BALF T cells of IPF patients (13). Moreover, the different conserved amino acids in the CDR3 region between DM and PM patients suggest that antigens recognized by BALF T cells might be different from each other.

While some T cells clonally accumulate through antigen stimulation, many other T cells polyclonally expand by interleukin (IL)-2 stimulation. What are the antigens recognized by clonally expanded T cells? To our knowledge, there are no reports on antigens for BALF T cells in myositis, whereas heat-shock proteins or viral antigens are possible candidates for T cells in muscles of PM patients (15). The antigens might be different from those in patients with sarcoidosis, because the TCR BV gene repertoire is not skewed but heterogeneous (8-10). Moreover, antigens should not be the same as those in IPF patients (13), because of the distinct conserved amino acid motifs in the TCR CDR3 region. BALF-specific T cell clones suggest that the antigens might be pulmonary antigens, e.g., autoantigens in alveolar epithelial cells or extracellular proteins such as viral or bacterial particles. Further studies on the antigens recognized by BALF T cells in PM/DM patients are necessary to clarity the role of T cells in the pathogenesis of myositis.

The autoaggressive $CD8^+$ T cells seem to attack myocytes as cytotoxic T cells in a perforin-dependent manner. The majority of BALF T cells are CD8-positive similar to those infiltrating muscles, suggesting that BALF T cells may function as cytotoxic T cells against pulmonary epithelial cells and result in lung fibrosis. It is considered that PM and DM are pathogenetically different. In DM, there is no report that clonal expansion of T cells in the muscle is noted. Our results did not identify it clearly, but showed similar clonal expansion of T cells in BALF between PM and DM. This is considerable, therefore we need additional experimental data. However, the appropriate treatment for pulmonary fibrosis in patients with PM/DM is still non-specific therapy such as corticosteroid and immunosuppressant. Therefore, detection of clonally expanded T cells in BALF should be the first step in the development of specific regulators of cytotoxic T cells that induce interstitial pneumonitis in PM/DM patients.

In conclusion, we demonstrated clonal accumulation of BALF T cells in PM/DM patients with IP, suggesting that T cells in the lung expand via antigen-driven stimulation. Although the autoantigens recognized by pulmonary T cells have not yet been identified, we believe our results will be potentially useful for the design of new treatment strategies against IP in PM/DM patients that are specifically designed to target T cells and antigens.

Acknowledgments

We thank Ms. Eriko Onose for the excellent technical assistance.

References

1. Haslam PL, Turton CW, Lukoszik A, Salsbury AJ, Dewar A, Collins JV and Turner-Warwickl M: Bronchoalveolar lavage fluid cell counts in cryptogenic fibrosing alveolitis and relation to therapy. Thorax 35: 328-339, 1980.
2. Haslam PL, Turton CW, Heard B, Lukoszik A, Salsbury AJ, Dewar A and Turner-Warwickl M: Bronchoalveolar lavage in pulmonary fibrosis: comparison of cells obtained with lung biopsy and clinical features. Thorax 35: 9-18, 1980.
3. Paliard X, West SG, Lafferty JA, Clements JR, Kappler JW, Marrack P and Kotzin BL: Evidence for the effects of a super antigen in rheumatoid arthritis. Science 253: 325-328, 1991.
4. Sumida T, Yonaha F, Maeda T, *et al*: T cell receptor repertoire of infiltrating T cells in lips of Sjögren's syndrome patients. J Clin Invest 89: 681-685, 1992.
5. Yonaha F, Sumida T, Maeda T, Tomioka H, Koike T and Yoshida S: Restricted junctional usage of T cell receptor Vß and Vß13 genes, which are overrepresented on infiltrating T cells in the lips of patients with Sjögren's syndrome. Arthritis Rheum 35: 1362-1367, 1992.
6. Kotzin BL, Karuturi S, Chou YK, *et al*: Preferential T-cell receptor beta-chain variable gene use in myelin basic protein-reactive T-cell clones from patients with multiple sclerosis. Proc Natl Acad Sci USA 88: 9161-9165, 1991.
7. Wucherpfening KW, Ota K, Endo N, Seidman JG, Rosenzweig A, Weiner HL and Hafler DA: Shared human T cell receptor V beta usage to immunodominant regions of myelin basic protein. Science 248: 1016-1019, 1990.
8. Moller DR, Konishi K, Kirby M, Balbi B and Crystal RG: Bias toward use of specific T cell receptor beta-chain variable region in a subgroup of individuals with sarcoidosis. J Clin Invest 82: 1183-1191, 1988.
9. Zissel G, Baumer I, Fleischer B, Schlaak M and Muller-Quernheim J: TCR V beta families in T cell clones from sarcoid lung parenchyma, BAL, and blood. Am J Respir Crit Care Med 156: 1593-1600, 1997.
10. Bellocq A, Lecossier D, Pierre-Audigier C, Tazi A, Valeyre D and Hance AJ: T cell receptor repertoire of T lymphocytes recovered from the lung and blood of patients with sarcoidosis. Am J Respir Crit Care Med 149: 646-654, 1994.
11. Hodges E, Dasmahapatra J, Smith JL, *et al*: T cell receptor Vß gene usage in bronchoalveolar lavage and peripheral blood T cells from asthmatic and normal subjects. Clin Exp Immunol 112: 363-374, 1998.
12. Umibe T, Kita Y, Nakao A, *et al*: Clonal expansion of T cells infiltrating in the airways of non-atopic asthmatics. Clin Exp Immunol 119: 390-397, 2000.
13. Shimizudani N, Murata H, Keino H, *et al*: Conserved CDR3 region of T cell receptor BV gene in lymphocytes from broncho-alveolar lavage fluid of patients with idiopathic pulmonary fibrosis. Clin Exp Immunol 129: 140-149, 2002.

14. Yamamoto K, Sakoda H, Nakajima T, *et al*: Accumulation of multiple T cell clonotypes in the synovial lesions of patients with rheumatoid arthritis revealed by a novel clonality analysis. Int Immunol 4: 1219-1223, 1992.
15. Mantegaazza R, Andreetta F, Bernasconi P, *et al*: Analysis of T cell receptor repertoire of muscle-infiltrating T lymphocytes in polymyositis. J Clin Invest 91: 2880-2886, 1993.
16. O'Hanlon TP, Dalakas MC, Plots PH and Miller FW: Predominant TCR-αß variable and joining gene expression by muscle-infiltrating lymphocytes in the idiopathic inflammatory myopathies. J Immunol 152: 2569-2576, 1994.
17. Lindberg C, Oldfors A and Tarkowski A: Restricted use of T cell receptor V genes in endomysial infiltrates of patients with inflammatory myopathies. Eur J Immunol 24: 2659-2663 1994.
18. Bender A, Ernst N, Iglesias A, Dornmair K, Wekerle H and Hohlfeld R: T cell receptor repertoire in polymyositis: clonal expansion of autoaggressive $CD8^+$ T cells. J Exp Med 181: 1863-1868, 1995.
19. Benveniste O, Cherin P, Maisonobe T, *et al*: Severe perturbations of the blood T cell repertoire in polymyositis, but not dermatomyositis patients. J Immunol 167: 3521-3529, 2001.
20. Nishio J, Suzuki M, Miyasaka N and Kohsaka H: Clonal biases of peripheral CD8 T cell repertoire directly reflect local inflammation in polymyositis. J Immunol 167: 4051-4058, 2001.
21. Hofbauer M, Wiesener S, Babbe H, *et al*: Clonal tracking of autoaggressive T cells in polymyositis by combining laser microdissection, single-cell PCR, and CDR3-spectratype analysis. Proc Natl Acad Sci USA 100: 4090-4095, 2003.
22. Bohan A and Peter JB: Polymyositis and dermatomyositis. N Engl J Med 292: 403-407, 1975.

Involvement of Regulatory T Cells in the Experimental Autoimmune Encephalomyelitis-Preventive Effect of Dendritic Cells Expressing Myelin Oligodendrocyte Glycoprotein plus TRAIL[1]

Shinya Hirata, Hidetake Matsuyoshi, Daiki Fukuma, Akari Kurisaki, Yasushi Uemura, Yasuharu Nishimura,[2] and Satoru Senju[2,3]

We previously reported the protection from myelin oligodendrocyte glycoprotein (MOG)-induced experimental autoimmune encephalomyelitis (EAE) by the adoptive transfer of genetically modified embryonic stem cell-derived dendritic cells (ES-DC) presenting MOG peptide in the context of MHC class II molecules and simultaneously expressing TRAIL (ES-DC-TRAIL/MOG). In the present study, we found the severity of EAE induced by another myelin autoantigen, myelin basic protein, was also decreased after treatment with ES-DC-TRAIL/MOG. This preventive effect diminished, if the function of $CD4^+CD25^+$ regulatory T cells (Treg) was abrogated by the injection of anti-CD25 mAb into mice before treatment with ES-DC-TRAIL/MOG. The adoptive transfer of $CD4^+CD25^+$ T cells from ES-DC-TRAIL/MOG-treated mice protected the recipient mice from MOG- or myelin basic protein-induced EAE. The number of $Foxp3^+$ cells increased in the spinal cords of mice treated with ES-DC-TRAIL/MOG. In vitro experiments showed that TRAIL expressed in genetically modified ES-DC and also in LPS-stimulated splenic macrophages had a capacity to augment the proliferation of $CD4^+CD25^+$ T cells. These results suggest that the prevention of EAE by treatment with ES-DC-TRAIL/MOG is mediated, at least in part, by MOG-reactive $CD4^+CD25^+$ Treg propagated by ES-DC-TRAIL/MOG. For the treatment of organ-specific autoimmune diseases, induction of Treg reactive to the organ-specific autoantigens by the transfer of DC-presenting Ags and simultaneously overexpressing TRAIL therefore appears to be a promising strategy. *The Journal of Immunology,* **2007, 178: 918–925.**

For the treatment of subjects with autoimmune and allergic diseases, it is desirable to down-modulate the immune response in an Ag-specific manner while not causing systemic immune suppression. To achieve this goal, genetically modified dendritic cells (DC)[4] presenting target Ags and simultaneously expressing immunoinhibitory molecules would be an attractive strategy (1).

TRAIL, a member of the TNF superfamily, is expressed in a variety of cell types, including lymphocytes, NK cells, NKT cells, and virus-infected APCs (2–5). The abrogation of functional TRAIL by gene targeting or the in vivo administration of soluble death receptor 5, one of receptors for TRAIL, results in the acceleration of autoimmune diseases in mouse models, for example collagen-induced arthritis, autoimmune diabetes, and experimental autoimmune encephalomyelitis (EAE) (6–9). It is thus evident that TRAIL plays a critical role in the regulation of the immune response or the maintenance of immunological self-tolerance to prevent autoimmunity. However, the precise mechanism for this has not yet been clarified regarding how TRAIL exerts such an effect.

We recently reported the protection from myelin oligodendrocyte glycoprotein (MOG)-induced EAE with genetically modified DC expressing MOG peptide along with TRAIL or programmed death-1 ligand (PD-L1) (1). For the genetic modification of DC, we used a method to generate DC from mouse embryonic stem cells in vitro (ES-DC) (10–13). For the efficient presentation of MOG peptide in the context of MHC class II molecules, we used an expression vector in which cDNA encoding for human MHC class II-associated invariant chain was mutated to contain antigenic peptide in the class II-associated invariant chain peptide region (14, 15). An epitope inserted into this vector is efficiently presented in the context of coexpressed MHC class II molecules. Based on these technologies, we generated transfectant ES-DC presenting MOG peptide and simultaneously expressing TRAIL or PD-L1, ES-DC-TRAIL/MOG, and ES-DC-PDL1/MOG, respectively.

The treatment of mice with either of the double-transfectant ES-DC significantly reduced the severity of MOG-induced EAE. In contrast, treatment with ES-DC expressing MOG alone, irrelevant Ag (OVA) plus TRAIL, or OVA plus PD-L1, or coinjection with ES-DC expressing MOG plus ES-DC expressing TRAIL or PD-L1, had no effect on the disease course. The immune response to irrelevant exogenous Ag (keyhole limpet hemocyanin) was not

Department of Immunogenetics, Graduate School of Medical Sciences, Kumamoto University, Kumamoto, Japan

Received for publication March 9, 2006. Accepted for publication October 31, 2006.

The costs of publication of this article were defrayed in part by the payment of page charges. This article must therefore be hereby marked *advertisement* in accordance with 18 U.S.C. Section 1734 solely to indicate this fact.

[1] This work was supported in part by Grants-in-Aid 12213111, 14370115, 14570421, 14657082, and the Program of Founding Research Centers for Emerging and Re-emerging Infectious Disease from the Ministry of Education, Science, Technology, Sports, and Culture, Japan, and a Research Grant for Intractable Diseases from the Ministry of Health, Labour and Welfare, Japan, and grants from the Uehara Memorial Foundation, and by funding from the Meiji Institute of Health Science.

[2] Y.N. and S.S. contributed equally to this study.

[3] Address correspondence and reprint requests to Dr. Satoru Senju, Department of Immunogenetics, Graduate School of Medical Sciences, Kumamoto University, Honjo 1-1-1, Kumamoto 860-8556, Japan. E-mail address: senjusat@gpo.kumamoto-u.ac.jp

[4] Abbreviations used in this paper: DC, dendritic cell; EAE, experimental autoimmune encephalomyelitis; MOG, myelin oligodendrocyte glycoprotein; ES, embryonic stem cell; PD-L1, programmed death-1 ligand; MBP, myelin basic protein; Treg, regulatory T cell; Tr1, T regulatory type 1.

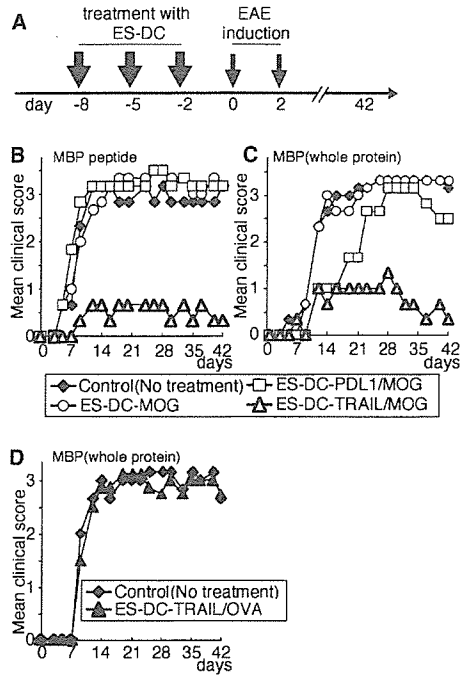

FIGURE 1. Prevention of MBP-induced EAE by treating the mice with ES-DC-TRAIL/MOG. *A*, The schedule for the pretreatment and induction of EAE is shown. CBF_1 mice (three to four mice per group) were i.p. injected with ES-DC (1×10^6 cells/mouse/injection) on days −8, −5, and −2. EAE was induced by the immunization of MBP peptide or whole protein on day 0, and the injection of *B. pertussis* toxin on days 0 and 2. *B–D*, The disease severity of mice immunized with MBP peptide (*B*) or whole protein (*C* and *D*) is shown. The data of all experiments are summarized in Table I.

impaired by treatment with any of the genetically modified ES-DC. These results suggest the possibility of treating autoimmune diseases without affecting immunity to exogenous Ags using genetically engineered DC presenting target autoantigen and simultaneously expressing TRAIL or PD-L1. In that study, we observed an increase in apoptosis of $CD4^+$ T cells in the spleens of mice treated with ES-DC-TRAIL/MOG, suggesting that protection from EAE by ES-DC-TRAIL/MOG is mediated by induction of apoptosis of MOG-reactive pathogenic $CD4^+$ T cells. In the present study, we found that the severity of not only MOG- but also myelin basic protein (MBP)-induced EAE was reduced by treatment with ES-DC-TRAIL/MOG. Regarding the mechanism underlying this disease-preventive effect, we obtained several lines of evidence supporting that MOG-reactive $CD4^+CD25^+$ regulatory T cells (Treg) were activated or propagated by the transfer of ES-DC-TRAIL/MOG and that the prevention of EAE by treatment with ES-DC-TRAIL/MOG was mediated, at least in part, by Treg.

Materials and Methods

Mice and cells

CBA and C57BL/6 mice obtained from Clea Animal or Charles River Laboratories were kept under specific pathogen-free conditions. Male CBA and female C57BL/6 mice were mated to generate F_1 (CBF_1) mice and all in vivo experiments were done using CBF_1 mice, syngeneic to TT2 ES cells. The mouse experiments were approved by the Animal Research Committee of Kumamoto University.

The mouse ES cell line, TT2, derived from CBF_1 blastocysts, and OP9 were maintained as previously described (10). The induction of differentiation of ES cells into ES-DC and generation of transfectant ES-DC-TRAIL, ES-DC-PDL1, ES-DC-MOG, ES-DC-TRAIL/MOG, ES-DC-PDL1/MOG, and ES-DC-TRAIL/OVA was done as described previously (1).

Protein, cytokines, and Abs

The mouse MOG p35–55 (MEVGWYRSPFSRVVHLYRNGK) and mouse MBP p35-47 (TGILDSIGRFFSG) were synthesized using the F-moc method on an automatic peptide synthesizer (PSSM8; Shimadzu) and purified using HPLC. Recombinant mouse GM-CSF (PeproTech) was purchased. Rat anti-mouse CD25 mAb was produced by culturing the PC61.5.3 cell line in the CELLINE system (BD Biosciences) and was purified by the MAbTrap kit (Amersham Biosciences). Abs and reagents used for staining were PE-conjugated anti-mouse CD25 (clone 3C7, rat IgG2b; BD Pharmingen) and FITC-conjugated anti-mouse CD4 (clone GK1.5, rat IgG2b; BD Pharmingen).

Induction of EAE and treatment with ES-DC

For the induction of EAE, 6- to 8-wk-old female CBF_1 mice were immunized by performing a s.c. injection at the base of tail with a 0.2-ml IFA/PBS solution containing 600 μg of MOG p35–55 peptide, MBP p35–47 peptide, or whole bovine MBP (Sigma-Aldrich), and 400 μg of *Mycobacterium tuberculosis* H37Ra (Difco Laboratories) on day 0. In addition, 500 ng of purified *Bordetella pertussis* toxin (Calbiochem) was injected i.p. on days 0 and 2 (1). For the prevention of EAE, mice were injected i.p. with ES-DC (1×10^6 cells/mouse/injection) on days −8, −5, and −2 (preimmunization treatment), or on days 14, 17, and 21 (postonset treatment). In some experiments, $CD25^+$ T cells were depleted by i.p. injections of anti-mouse CD25 mAb (clone PC61.5.3) as described (16). In brief, the mAb (400 μg/mouse) was administrated on days −28, −24, −21, and −14. Depletion was verified by staining PBMC and then analyzing them on a flow cytometer (FACScan; BD Biosciences). The mice were observed over a period of 42 or 56 days (postonset treatment) for clinical signs and scores were assigned based on the following scale: 0, normal; 1, weakness of the tail and/or paralysis of the distal half of the tail; 2, loss of tail tonicity and abnormal gait; 3, weakly partial hind-limb paralysis; 3.5, strongly partial

Table I. *Suppression of MBP-induced EAE induction in CBF_1 mice treated with ES-DC expressing MOG plus TRAIL*[a]

Treatment (ES-DC) of Mice	EAE Induced with	Disease Incidence	Day of Onset	Mean Peak Clinical Score
No treatment (control)	MBP pep	12/12	6.4 ± 1.3	3.1 ± 0.1
TRAIL/MOG	MBP pep	2/6	8.0 ± 1.0	0.7 ± 0.9
PD-L1/MOG	MBP pep	6/6	8.0 ± 2.7	3.4 ± 0.1
MOG	MBP pep	3/3	6.3 ± 1.8	3.5 ± 0.0
No treatment (control)	MBP whole	15/15	9.4 ± 1.5	3.1 ± 0.2
TRAIL/MOG	MBP whole	5/9	15.2 ± 4.6	1.0 ± 0.9
PD-L1/MOG	MBP whole	6/6	13.5 ± 3.3	3.1 ± 0.1
MOG	MBP whole	6/6	11.7 ± 0.6	3.2 ± 0.2
TRAIL/OVA	MBP whole	4/4	9.8 ± 1.1	3.3 ± 0.3
CD25 depl.[b] plus no treatment	MBP whole	6/6	10.1 ± 1.2	3.8 ± 0.5
CD25 depl.[b] plus TRAIL/MOG	MBP whole	8/8	10.0 ± 1.5	4.3 ± 1.0

[a] The data are combined from a total of nine separate experiments including those shown in Figs. 1 and 4.

[b] In these mice, $CD25^+$ cells were depleted by the treatment with anti-CD25 mAb and subsequently mice were transferred with ES-DC or left untreated. The values of onset day and mean peak clinical score are rounded off to the first decimal place.

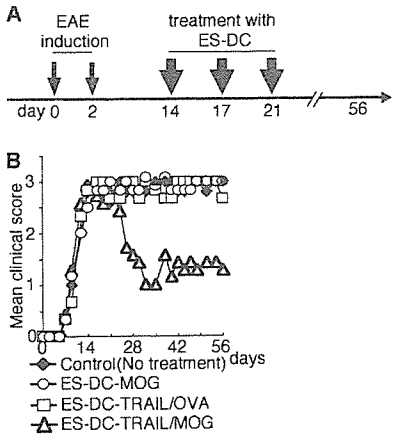

FIGURE 2. Inhibition of MBP-induced EAE by treating the mice with ES-DC-TRAIL/MOG. *A*, The schedule for induction of EAE and treatment is shown. CBF_1 mice (five to seven mice per group) were immunized on days 0 and 2 according to the EAE-induction schedule described above, and subsequently i.p. injected with ES-DC (1×10^6 cells/mouse/injection) on days 14, 17, and 21. *B*, The disease severity of mice immunized with MBP whole protein is shown.

hind-limb paralysis; 4, complete hind-limb paralysis; 5, fore-limb paralysis or moribundity; 6, death.

Adoptive transfer of T cells

For the adoptive transfer experiments, donor CBF_1 mice were i.p. injected with ES-DC (1×10^6 cells/injection/mouse) on days -10, -7, and -4. $CD4^+$ T cells and $CD4^+CD25^+$ T cells were isolated from the spleen cells of donor mice using the MACS cell sorting system (Miltenyi Biotec). For the isolation of $CD4^+$ T cells, non-$CD4^+$ T cells magnetically labeled with a biotin-conjugated Ab mixture (anti-CD8α, anti-CD11b, anti-CD45R, anti-DX5, and anti-Ter-119) and anti-biotin microbeads were depleted on an autoMACS cell separator. Subsequently, $CD25^+$ T cells, labeled with anti-CD25 mAb conjugated with PE and anti-PE microbeads, were isolated from the $CD4^+$ T cell fraction using positive sorting columns. Cell purity was checked by FACS analysis: $CD4^+$ T cells were >95% after the first step and $CD4^+CD25^+$ cells were >95% after the second step. The $CD4^+$ T cells, $CD4^+CD25^+$ T cells, or $CD4^+CD25^-$ T cells were i.v. injected into recipient mice (2.5×10^6, 3×10^5, or 2.2×10^6 cells/mouse, respectively) on day -2. The recipient mice were subjected to EAE induction (on days 0 and 2) as described above.

Proliferation assay of Treg

Mouse $CD4^+CD25^+$ Treg were purified with a Treg separation kit (MACS) from the spleen cells of naive CBF_1 mice as described above. Assay for the proliferation of Treg was done, as described previously (17). In brief, 1×10^4 ES-DC or syngeneic splenic macrophages were x-ray irradiated (25 Gy), and cocultured with 1×10^4 Treg in the presence of anti-CD3 mAb (clone 145-2C11, 1 μg/ml) and human IL-2 (10–30 U/ml) in wells of 96-well round-bottom culture plates. In some assay, anti-TRAIL mAb (clone N2B2 (5 μg/ml); eBioscience) was added. Splenic macrophages were prepared by collecting plastic dish-adherent cells. The cells were cultured for 3 days, and [^{3}H]thymidine (6.7 Ci/mM) was added to the culture (1 μCi/well) in the last 12 h. At the end of culture, cells were harvested onto glass fiber filters (Wallac) and the incorporation of [^{3}H]thymidine was measured by scintillation counting. The expression of TRAIL in LPS-stimulated spleen cells and macrophages was confirmed by RT-PCR, as described previously (1). The relative quantity of cDNA in each sample was first normalized by PCR for G3PDH. The primer sequences were as follows: TRAIL, 5′-AACCCTCTAGACCGCCGCCACCATGCCTTCCTCAGGGG CCCTGAA-3′ and 5′-GAAATGGTGTCCTGAAAGGTTC; G3PDH, 5′-GG AAAGCTGTGGCGTGATG-3′ and 5′-CTGTTGCTGTAGCCGTATTC-3′.

Immunohistochemical analysis

Freshly excised spinal cords were immediately frozen and embedded in Tissue-Tek OCT compound (Sakura Fine Technical). Immunohistochemical staining of Foxp3 and CD4 was done, as previously described (1, 12), but with some modification. In brief, serial 7-μm sections were made using cryostat and underwent immunochemical staining with anti-Foxp3 mAb

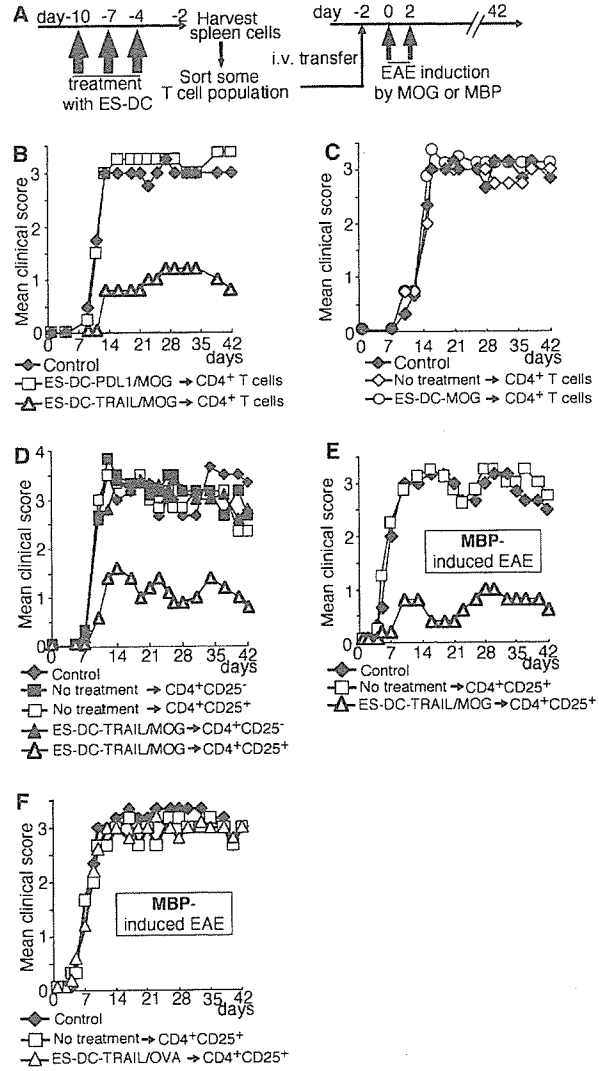

FIGURE 3. Protection from MOG or MBP-induced EAE by the adoptive transfer of $CD4^+CD25^+$ T cells from the mice treated with ES-DC expressing MOG plus TRAIL. *A*, The schedule for the treatment of donor mice with ES-DC, the adoptive transfer of some population of T cells, and the induction of EAE in the recipient mice are shown. The donor CBF_1 mice were i.p. injected with ES-DC (1×10^6 cells/mouse/injection) on days -10, -7, and -4. The T cells were isolated from the donor mice and then transferred to naive mice on day -2. The recipient mice were immunized with MOG peptide (*B–D*) or MBP whole protein (*E* and *F*) on days 0 and 2 according to the EAE-induction protocol as shown in Fig. 1. *B* and *C*, The disease severity of the mice transferred with $CD4^+$ T cells (2.5×10^6 cells/mouse) from ES-DC-TRAIL/MOG, ES-DC-PD-L1/MOG, ES-DC-MOG, ES-DC-TRAIL/OVA-treated mice, or naive mice is shown. *D–F*, The disease severity of the mice transferred with $CD4^+CD25^+$ T cells or $CD4^+CD25^-$ T cells (3×10^5 or 2.2×10^6 cells/mouse, respectively) from ES-DC-TRAIL/MOG-treated mice or naive mice is shown. Control mice were injected with RPMI 1640 medium alone without T cells. The data of all experiments are summarized in Table II.

(clone FJK-16s, rat IgG2a; eBioscience) or CD4 (clone L3T4; BD Pharmingen), and N-Histofine Simple Stain Mouse MAX PO (Nichirei).

Statistical analysis

The two-tailed Student's *t* test was used to determine any statistical significance of differences. A value of $p < 0.05$ was considered to indicate statistical significance (15). The values indicated in tables are rounded off to the first decimal place.

Table II. *Suppression of EAE induction by adoptive transfer of T cells from CBF$_1$ mice treated with ES-DC expressing MOG plus TRAIL*[a]

Treatment (ES-DC) of Donor Mice	T Cells Transferred	EAE Induction	Disease Incidence	Day of Onset	Mean Peak Clinical Score
	No transfer	MOG pep	14/14	10.3 ± 1.3	3.6 ± 0.4
TRAIL/MOG	$CD4^+$	MOG pep	3/7	12.3 ± 0.9	1.0 ± 1.1
PD-L1/MOG	$CD4^+$	MOG pep	4/4	10.5 ± 0.8	3.4 ± 0.2
MOG	$CD4^+$	MOG pep	4/4	11.3 ± 1.9	3.4 ± 0.4
No treatment	$CD4^+$	MOG pep	4/4	11.3 ± 1.9	3.0 ± 0.0
TRAIL/MOG	$CD4^+CD25^+$	MOG pep	5/7	14.4 ± 4.2	1.7 ± 1.0
TRAIL/MOG	$CD4^+CD25^-$	MOG pep	7/7	9.0 ± 1.1	3.4 ± 0.2
No treatment	$CD4^+CD25^+$	MOG pep	3/3	9.0 ± 1.3	3.7 ± 0.2
No treatment	$CD4^+CD25^-$	MOG pep	3/3	9.0 ± 1.3	3.8 ± 0.2
	No transfer	MBP pep	18/18	6.4 ± 1.3	3.1 ± 0.1
TRAIL/MOG	$CD4^+CD25^+$	MBP pep	3/8	13.0 ± 8.7	0.8 ± 0.9
TRAIL/OVA	$CD4^+CD25^+$	MBP pep	8/8	6.1 ± 1.4	3.1 ± 0.2
No treatment	$CD4^+CD25^+$	MBP pep	7/7	5.7 ± 1.1	3.1 ± 0.1

[a] The data are combined from a total of 10 separate experiments, including those shown in Fig. 3. The values of onset day and mean peak clinical score are rounded off to the first decimal place.

Results

Prevention of MBP-induced EAE by the transfer of ES-DC genetically engineered to express MOG peptide along with TRAIL

We recently demonstrated the prevention of MOG-induced EAE by treatment with ES-DC expressing MOG peptide plus TRAIL (ES-DC-TRAIL/MOG) or MOG peptide plus PD-L1 (ES-DC-PDL1/MOG). Regarding the mechanism for preventing EAE by the genetically modified ES-DC, we considered not only the possibility of the direct down-modulation of MOG-reactive effector T cells such as the induction of anergy or apoptosis, but also the possibility of promoting MOG-reactive T cells with regulatory or immune-suppressive functions. We hypothesized that, if the latter had been the case, then pretreatment with ES-DC-TRAIL/MOG or ES-DC-PDL1/MOG may thus have had some preventive effect on not only MOG- but also MBP-induced EAE. To test this possibility, we pretreated mice with ES-DC-TRAIL/MOG or ES-DC-PDL1/MOG and subjected them to EAE induction by immunization with MBP (whole protein) or MBP p35-47, according to the schedule depicted in Fig. 1*A*. As a result, we found the severity of both MBP whole protein- and peptide-induced EAE to be significantly reduced by pretreatment with ES-DC-TRAIL/MOG. In contrast, pretreatment with ES-DC-PDL1/MOG, ES-DC-TRAIL/OVA (as irrelevant Ag), and ES-DC-MOG had no effect on MBP-induced EAE (Fig. 1, *B–D*, and Table I).

Next, we tested whether treatment with ES-DC after the onset of MBP-induced EAE would achieve some suppressive effect on the course of disease. The mice immunized according to the protocol for MBP-induced EAE were injected with ES-DC on days 14, 17, and 21 (1×10^6 cells/mouse/injection) as shown in Fig. 2*A*. Even in this postonset treatment, injection of ES-DC-TRAIL/MOG reduced severity of the disease, while ES-DC-TRAIL/OVA and ES-DC-MOG did not do so (Fig. 2*B*).

Prevention of MOG- and MBP-induced EAE by the adoptive transfer of $CD4^+CD25^+$ T cells from the mice treated with ES-DC-TRAIL/MOG

We considered the possibility that MOG-reactive T cells possessing some immunoregulatory effect were activated or propagated by the transferred ES-DC-TRAIL/MOG and that the T cells exerted a protective effect against MBP-induced EAE. To address this possibility, we performed adoptive transfer experiments. We isolated $CD4^+$ T cells from the spleens of the donor mice treated with ES-DC and transferred them into naive recipient mice. Subsequently, the recipient mice were subjected to an immunization procedure for MOG-induced EAE (Fig. 3*A*). As shown in Fig. 3, *B* and *C*, and Table II, the transfer of 2.5×10^6 $CD4^+$ T cells isolated from the mice treated with ES-DC-TRAIL/MOG significantly reduced the severity of EAE of the recipient mice. In contrast, $CD4^+$ T cells isolated from the mice treated with ES-DC-PDL1/MOG or ES-DC-MOG or those from untreated mice showed no effect. These results support the notion that $CD4^+$ T cells with some regulatory activity were induced, activated, or propagated by the treatment with ES-DC-TRAIL/MOG.

Several types of $CD4^+$ T cells with a potential for reducing the severity of Th1 cell-mediated autoimmune diseases are known, such as T regulatory type 1 (Tr1) cells, Th2 cells, or $CD4^+CD25^+$ Treg. To identify the type of T cells involved in the disease-preventive effect, we separated $CD4^+$ T cells isolated from ES-DC-TRAIL/MOG-treated mice into $CD4^+CD25^+$ and $CD4^+CD25^-$ T cells before transfer. In CBF$_1$ mice, 10–15% of splenic $CD4^+$ T cells were $CD25^+$ (data not shown), thus indicating that 2.5×10^6 $CD4^+$ T cells include $\sim 3 \times 10^5$ $CD25^+$ T cells and 2.2×10^6 $CD25^-$ T cells. Therefore, we transferred 3×10^5 $CD25^+$ T cells and 2.2×10^6 $CD25^-$ T cells into separate mice. As shown in Fig. 3*D* and Table II, the transfer of 3×10^5 $CD4^+CD25^+$ T cells isolated from mice treated with ES-DC-TRAIL/MOG significantly reduced the severity of MOG-induced EAE in the recipient mice. In contrast, the transfer of $CD4^+CD25^+$ or $CD4^+CD25^-$ T cells from naive mice or $CD4^+CD25^-$ T cells from ES-DC-TRAIL/MOG-treated mice had no effect. These results indicate that $CD25^+$ T cells among the $CD4^+$ T cells were responsible for the above-described protective effect of ES-DC-TRAIL/MOG against EAE.

We next tested whether the transfer of $CD4^+CD25^+$ T cells isolated from donor mice treated with ES-DC-TRAIL/MOG would have any effect on MBP-induced EAE. We transferred $CD4^+CD25^+$ T cells from the donor mice treated with ES-DC as described above. Subsequently, the recipient mice were subjected to an immunization procedure for MBP-induced EAE. As shown in Fig. 3, *E* and *F*, and Table II, the transfer of 3×10^5 $CD4^+CD25^+$ T cells isolated from mice treated with ES-DC-TRAIL/MOG significantly reduced the severity of MBP-induced EAE in the recipient mice, but the transfer of $CD4^+CD25^+$ T cells isolated from ES-DC-TRAIL/OVA-treated mice or naive mice did not do so. These results indicate that ES-DC-TRAIL/MOG-

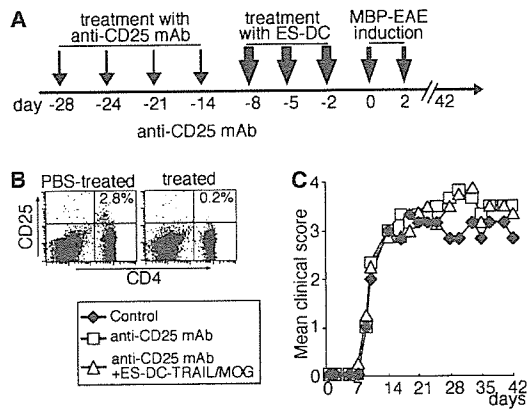

FIGURE 4. The depletion of $CD4^+CD25^+$ T cells diminished the preventive effect of ES-DC-TRAIL/MOG on MBP-induced EAE. *A*, The schedule for the depletion with anti-CD25 mAb, pretreatments with ES-DC, and induction of EAE are shown. CBF_1 mice (three to four mice per group) were i.p. injected with anti-mouse CD25 mAb (400 μg/mouse/injection) on days −28, −24, −21, −14 and then were treated with ES-DC (1×10^6 cells/mouse/injection) on days −8, −5, and −2. EAE was induced by immunization with MBP whole protein on days 0 and 2 as in Fig. 1. *B*, $CD4^+CD25^+$ cells of peripheral blood of anti-CD25 mAb-treated (*right*) and PBS-treated control (*left*) mice were analyzed by flow cytometry on day −2. The percentage of $CD4^+CD25^+$ cells among $CD4^+$ cells is shown. *C*, The severity of MBP-induced EAE is shown. Control mice were injected with PBS alone without Ab and RPMI 1640 medium alone without ES-DC. The data of all experiments are summarized in Table I.

induced $CD4^+CD25^+$ T cells had a protective effect against not only MOG- but also MBP-induced EAE.

Protection from MBP-induced EAE by ES-DC-TRAIL/MOG depends on $CD25^+$ cells

To further verify the involvement of $CD4^+CD25^+$ T cells in the disease-preventive effect of ES-DC-TRAIL/MOG, we performed depletion experiments of $CD4^+CD25^+$ T cells. We injected the mice with anti-mouse CD25 mAb four times on days −28, −24, −21, and −14 (Fig. 4*A*). Depletion of $CD4^+CD25^+$ T cells was confirmed by flow cytometry analysis of PBLs. $CD25^+$ cells were $0.3 \pm 0.1\%$ of $CD4^+$ T cells in anti-CD25 mAb-treated mice ($n = 4$), whereas they were $2.6 \pm 0.3\%$ in control (PBS-injected) mice ($n = 3$). Representative results of flow cytometry analysis are shown in Fig. 4*B*. Thereafter, we treated the mice with ES-DC-TRAIL/MOG and then immunized them with MBP according to the EAE induction protocol. As shown in Fig. 4*C* and Table I, the effect of ES-DC-TRAIL/MOG to prevent MBP-induced EAE completely disappeared in the mice in which the $CD4^+CD25^+$ T cells were depleted. These results further support the possibility that the prevention of MBP-induced EAE by ES-DC-TRAIL/MOG was mediated by $CD4^+CD25^+$ T cells. In addition, treatment with anti-CD25 mAb slightly worsened the disease course even when mice were not treated with ES-DC, suggesting that $CD4^+CD25^+$ T cells ameliorate the disease to some extent in the natural course after EAE induction.

Increased number of $Foxp3^+$ cells infiltrating into spinal cords of mice treated with ES-DC-TRAIL/MOG

At present, Foxp3 is the most reliable molecular marker for Treg (18). We performed immunohistochemical analysis to detect $Foxp3^+$ cells in the spinal cord of mice treated with ES-DC. We treated the mice with ES-DC and then immunized them with MOG according to the EAE induction protocol. On day 11, the spinal cords harvested from mice were stained with anti-Foxp3 mAb (Fig. 5, *A–C*) and anti-CD4 mAb, and $Foxp3^+$ cells and $CD4^+$ cells were counted. As shown in Fig. 5*D*, the infiltration of $Foxp3^+$ cells into the spinal cord was enhanced in mice treated with ES-DC-TRAIL/MOG, compared with mice with no treatment or mice treated with ES-DC-PDL1/MOG. In contrast, the infiltration of $CD4^+$ cells into the spinal cords was reduced in mice treated with ES-DC-TRAIL/MOG or ES-DC-PDL1/MOG, compared with the observation in mice with no treatment. These results further support the notion of involvement of Treg in the disease-protection effect.

Enhanced capacity of ES-DC expressing TRAIL to induce the in vitro proliferation of naive $CD4^+CD25^+$ Tregs

Recent studies have demonstrated that bone marrow-derived DC and splenic DC have a potent capacity to promote the proliferation of $CD4^+CD25^+$ Treg both in vitro and in vivo (17, 19). We investigated whether ES-DC had the capacity to promote the proliferation of $CD4^+CD25^+$ Treg and also whether the expression of TRAIL had any effect on this capacity of ES-DC. Treg isolated from spleen of naive CBF_1 mice were cocultured with ES-DC in the presence of anti-CD3 mAb (1 μg/ml) and a low dose of human IL-2 (10 U/ml). As shown in Fig. 6*A*, all three types of ES-DC, nontransfectant ES-DC, ES-DC-TRAIL, or ES-DC-PDL1, induced a proliferation of Treg more potently than splenic macrophages. The increased proliferation of Treg was observed upon coculture with ES-DC-TRAIL, in comparison to that with other

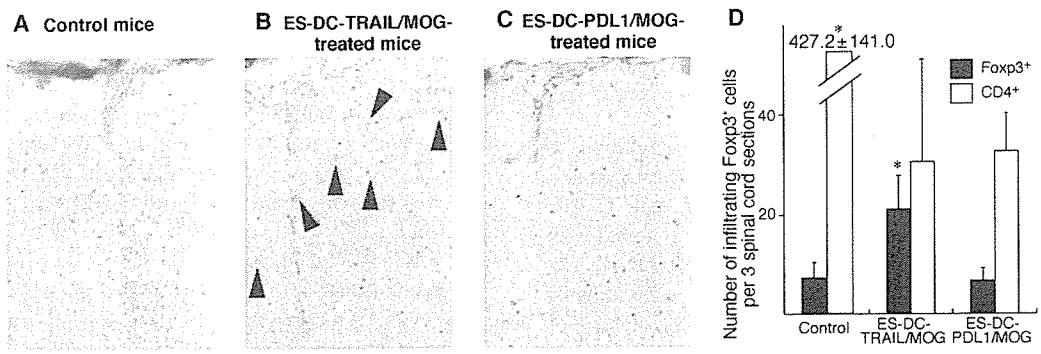

FIGURE 5. Increased number of $Foxp3^+$ cells in spinal cords of mice treated with ES-DC expressing MOG plus TRAIL. CBF_1 mice (five mice per group) were pretreated with ES-DC-TRAIL/MOG or PDL1/MOG (1×10^6 cells/mouse/injection) as in Fig. 1 or left untreated. Subsequently, EAE was induced by immunization with MOG peptide on days 0 and 2. The cervical, thoracic, and lumbar spinal cord was isolated on day 11 and subjected to immunohistochemical analysis. The $Foxp3^+$ cells (*A–C*, arrowhead) and $CD4^+$ cells were stained and microscopically counted in three sections of spinal cord (*D*). Results are expressed as mean of samples obtained from five mice ± SD. *, The increase in number of infiltrated cells is statistically significant ($p < 0.01$) as compared with other groups.